Journal of Biomolecular Structure and Dynamics

ISSN: (Print) (Online) Journal homepage: https://www.tandfonline.com/loi/tbsd20

# Deleterious single nucleotide polymorphisms (SNPs) of human IFNAR2 gene facilitate COVID-19 severity in patients: a comprehensive *in silico* approach

**Shamima Akter, Arpita Singha Roy, Mahafujul Islam Quadery Tonmoy & Md Sajedul Islam**

**To cite this article:** Shamima Akter, Arpita Singha Roy, Mahafujul Islam Quadery Tonmoy & Md Sajedul Islam (2022) Deleterious single nucleotide polymorphisms (SNPs) of human IFNAR2 gene facilitate COVID-19 severity in patients: a comprehensive *in silico* approach, Journal of Biomolecular Structure and Dynamics, 40:21, 11173-11189, DOI: 10.1080/07391102.2021.1957714

**To link to this article:** https://doi.org/10.1080/07391102.2021.1957714

JOURNAL OF BIOMOLECULAR STRUCTURE AND DYNAMICS
2022, VOL. 40, NO. 21, 11173–11189
https://doi.org/10.1080/07391102.2021.1957714



# Deleterious single nucleotide polymorphisms (SNPs) of human IFNAR2 gene facilitate COVID-19 severity in patients: a comprehensive *in silico* approach

Shamima Akter[a], Arpita Singha Roy[b], Mahafujul Islam Quadery Tonmoy[b] and Md Sajedul Islam[c]

[a]Department of Bioinformatics and Computational Biology, George Mason University, Fairfax, VA, USA;[b]Department of Biotechnology and Genetic Engineering, Noakhali Science and Technology University, Noakhali, Bangladesh; [c]Department of Biochemistry & Biotechnology, University of Barishal, Barishal, Bangladesh

Communicated by Ramaswamy H. Sarma

**ABSTRACT**

In humans, the dimeric receptor complex IFNAR2-IFNAR1 accelerates cellular response triggered by type I interferon (IFN) family proteins in response to viral infection including Coronavirus infection. Studies have revealed the association of the *IFNAR2* gene with severe illness in Coronavirus infection and indicated the association of genomic variants, i.e. single nucleotide polymorphisms (SNPs). However, comprehensive analysis of SNPs of the *IFNAR2* gene has not been performed in both coding and non-coding region to find the causes of loss of function of IFNAR2 in COVID-19 patients. In this study, we have characterized coding SNPs (nsSNPs) of *IFNAR2* gene using different bioinformatics tools and identified deleterious SNPs. We found 9 nsSNPs as pathogenic and disease-causing along with a decrease in protein stability. We employed molecular docking analysis that showed 5 nsSNPs to decrease binding affinity to IFN. Later, MD simulations showed that P136R mutant may destabilize crucial binding with the IFN molecule in response to COVID-19. Thus, P136R is likely to have a high impact on disrupting the structure of the IFNAR2 protein. GTEx portal analysis predicted 14 sQTLs and 5 eQTLs SNPs in lung tissues hampering the post-transcriptional modification (splicing) and altering the expression of the *IFNAR2* gene. sQTLs and eQTLs SNPs potentially explain the reduced IFNAR2 production leading to severe diseases. These mutants in the coding and non-coding region of the *IFNAR2* gene can help to recognize severe illness due to COVID 19 and consequently assist to develop an effective drug against the infection.

**ARTICLE HISTORY**
Received 16 April 2021
Accepted 10 July 2021

**KEYWORDS**
SNPs; IFNAR2; COVID-19; molecular docking; protein–protein interaction; molecular dynamics simulation; GTEx

## 1. Introduction

In December 2019, severe acute respiratory syndrome coronavirus 2 (SARS-CoV-2) was first detected and quickly transmitted through individuals (humans) to individuals (WHO., 2020a, WHO., 2020b) in Wuhan, China. This outbreak of coronavirus disease (COVID-19) was subsequently described as a global pandemic by the World Health Organization (WHO., 2020a, WHO., 2020b ). An unprecedented shift has occurred in our lives due to COVID-19 disease. Sore throat, cough, fever, runny nose and breathing difficulties continue to be the significant symptoms, whereas some people are found to be asymptotic, which in turn speeds up the spread of the disease (Chen et al., 2020; Ren et al., 2020; Zhu et al., 2020). SARS-CoV-2 is a member of a large respiratory virus family that causes the severe acute respiratory syndrome (SARS) (Drosten et al., 2003). SARS-CoV-2 triggers the infection of lower respiratory tract along with extrapulmonary symptoms leading to severe illness in COVID-19. The lack of appropriate medications or treatments to fight effectively against this virus has made this disease dangerous and life-threatening. According to the COVID-19 Dashboard on March 29, 2021 by the Center for Systems Science and Engineering (CSSE) at Johns Hopkins University, over 127 million people in more than 200 countries have been infected and more than 2,785, 365 people were reported dead (Jennings, 2021). The clinical spectrum of this disease is very wide, as many individuals may be asymptomatic (accounting for up to 40%), while others suffer from severe COVID-19 disease with high fatality rate (Oran & Topol, 2020). The determinants of this spectrum need to be identified according to several studies (Bastard et al., 2020; Beck & Aksentijevich, 2020; Q. Zhang et al., 2020), where they emphasized to understand the mechanism and the causes of this disease. The persisting question is why this spectrum is so diverse and unpredictable.

Several studies revealed that the Type I interferon (IFN) signaling pathway plays a critical role in facilitating innate immune response against viral infections and protection against COVID-19 (LoPresti et al., 2020; Van Der Made et al., 2020). Genes of the Type I IFN pathway together with the Interferon alpha/beta receptor 2 (IFNAR2) receptor have been identified in some studies to elucidate the severity of the disease. Moreover, many studies described that if Type I IFN response is impaired, then severe COVID-19 infections

CONTACT Shamima Akter sakter5@gmu.edu Department of Bioinformatics and Computational Biology, George Mason University, Fairfax, VA 22030, USA.
Supplemental data for this article can be accessed online at http://doi.org/10.1080/07391102.2021.1957714.
This article has been republished with minor changes. These changes do not impact the academic content of the article.

arise (Arunachalam et al., 2020; Hadjadj et al., 2020; Lee & Shin, 2020). But why the Type I IFN signaling pathway is repressed remained unclear and actual determinants were unknown. Recently, a study revealed some promising factors in the IFN pathway and found out that *IFNAR2* and *TYK2* gene variants are associated with severe COVID-19 disease symptoms. Pairo-Castineira et al. showed evidence of the *IFNAR2* gene association through a GWAS study. They found evidence of a causal link with low expression of *IFNAR2* with the fatal condition of the disease using Mendelian randomization. Furthermore, researchers asserted that increased expression of IFNAR2 can reduce the critical illness due to COVID-19 (Pairo-Castineira et al., 2021). Thus, the study supported the protective role of IFNAR2 receptor in severely ill patients.

Susceptibility to respiratory infections becomes life-threatening and is found to be associated with specific genetic variants (Clohisey & Baillie, 2019). During viral pathogenesis including SARS-CoV-2, several genetic variants of the host cause loss of function in proteins associated with crucial immune responses that may lead to vigorous adverse symptoms in susceptible people (Pairo-Castineira et al., 2021). Moreover, another study has pointed out that genetic variants cause loss-of-function in the proteins of the Type I IFN pathway leading to severe immunodeficiency that results in life-threatening complications( Beck & Aksentijevich, 2020; Q. Zhang et al., 2020 ). They examined the patients with severe COVID-19 disease and found out rare pathogenic variants in 13 genes in the Type I IFN pathway including *IFNAR2*. Thus, variants of *IFNAR2* play a vital role in severe COVID-19 and many other viral diseases.

In the human genome, the most widespread category of genomic variations of a gene(s) are SNPs in the coding and non-coding region. Coding SNPs particularly non-synonymous (nsSNPs) replace amino acids in protein sequence and have a larger effect on the protein solubility, structure, function, and stability (Hamosh et al., 1992). These are characterized as either damaging/pathogenic (i.e. triggering disease attributes), or neutral/benign (i.e. no impact on protein structure and function) (Cargill et al., 1999; Czarny et al., 2018). The genomic basis of COVID-19 severity can be identified by distinguishing harmful nsSNPs from neutral nsSNPs in the *IFNAR2* gene. Consequently, this approach will assist in determining new medicinal target(s) to cure the disease. Therefore, the identification of deleterious nsSNPs in *IFNAR2* may recommend crucial information toward SARS-CoV-2 prevention.

Various bioinformatics tools are widely used to evaluate the damaging SNPs and the effect of these SNPs in the structure, stability, and function of a protein ( Desai & Chauhan, 2016; Divanshu et al., 2014; Nimir et al., 2017; M. Zhang et al., 2020 ). In another study, researchers have applied several computational tools along with molecular docking and MD simulations to predict SNPs of the human *STK11* gene (Islam et al., 2019). Utilizing *in silico* analysis, investigators projected that nsSNPs of the human RASSF5 gene possess detrimental impacts on protein function and structure (Hossain et al., 2020). In addition, scientists completed a comprehensive depiction of pathogenic coding and non-coding SNPs in the *TP63* gene and applied various *in silico* tools along with docking and MD simulations (Akter et al., 2021). These investigations enhance the application efficiency of bioinformatics tools examining and validating genetic modifications. Several other studies also implemented different *in silico* tools along with molecular docking and MD simulations to characterize nsSNPs in different genes (Abdul Samad et al., 2016; Chakraborty et al., 2018; Islam et al., 2019; Dash et al., 2020; Havranek & Islam, 2020; Owji et al., 2020) and to design drugs for COVID-19 (Bhardwaj et al., 2021; Ghosh et al., 2020a; Sharma et al., 2021).

Therefore, the objectives of the study include: (1) comprehensive characterization of numerous nsSNPs of the human *IFNAR2* gene by applying various bioinformatics algorithms (*in silico* tools), (2) analysis of the molecular dynamics simulation for significant nsSNPs of *IFNAR2 gene*, (3) analysis of the Molecular docking to distinguish the consequence of nsSNPs on binding affinity with other molecules/ligands using Autodock-Vina/PyRx, Chimera 1.13, (4) visualization of the impacts of nsSNPs by Chimera1.14, and (5) investigation of noncoding SNPs in *IFNAR2* gene utilizing GTEx portal, PolymiRTS, and RegulomeDB. The flow diagram depicting different activities of the study is shown in Figure 1.

## 2. Methods

### 2.1. Retrieval of SNPs data

In our study, the Ensemble genome browser was selected to examine and investigate the human *IFNAR2* gene (Ensembl, 2021) and the SNP data were collected by selecting the transcript that codes for the full-length IFNAR2 protein (515 a.a) (UniProt, 2021). Additionally, the dbSNP database (Sherry et al., 2001) was used as the SNPs data source for both coding and non-coding SNPs of IFNAR2 for all analysis.

### 2.2. Analysis of nsSNPs for functional consequences

*SIFT* (Sorting Intolerant From Tolerant), was employed to detect the deleterious nsSNPs in *IFNAR2*. To predict polymorphisms and mutants, SIFT can distinguish functional amino acids from deleterious ones. This program assumes that major amino acids are preserved and changes at some positions tend to be deleterious. Replacements are projected as deleterious or benign based on the standardized probability score (0.05 or lower predicted as deleterious/harmful and higher than 0.05 projected as tolerated/benign)(Sim et al., 2012). For SIFT prediction, individual amino acid replacements and rsID of each SNP of human *IFNAR2* gene were provided as the input.

To categorize and predict the functional effects of allele variations (SNPs), *PolyPhen2* (Polymorphism Phenotyping v2) (Adzhubei et al., 2010) employs Naive Bayes. PolyPhen2 assesses the site-specific sequence conservation assisted by the PSIC (position-specific independent count) and estimates the difference between the native and mutating variants. PolyPhen2 categorizes SNPs into three separate categories, (1) probably damaging (2) possibly damaging or 3) benign.

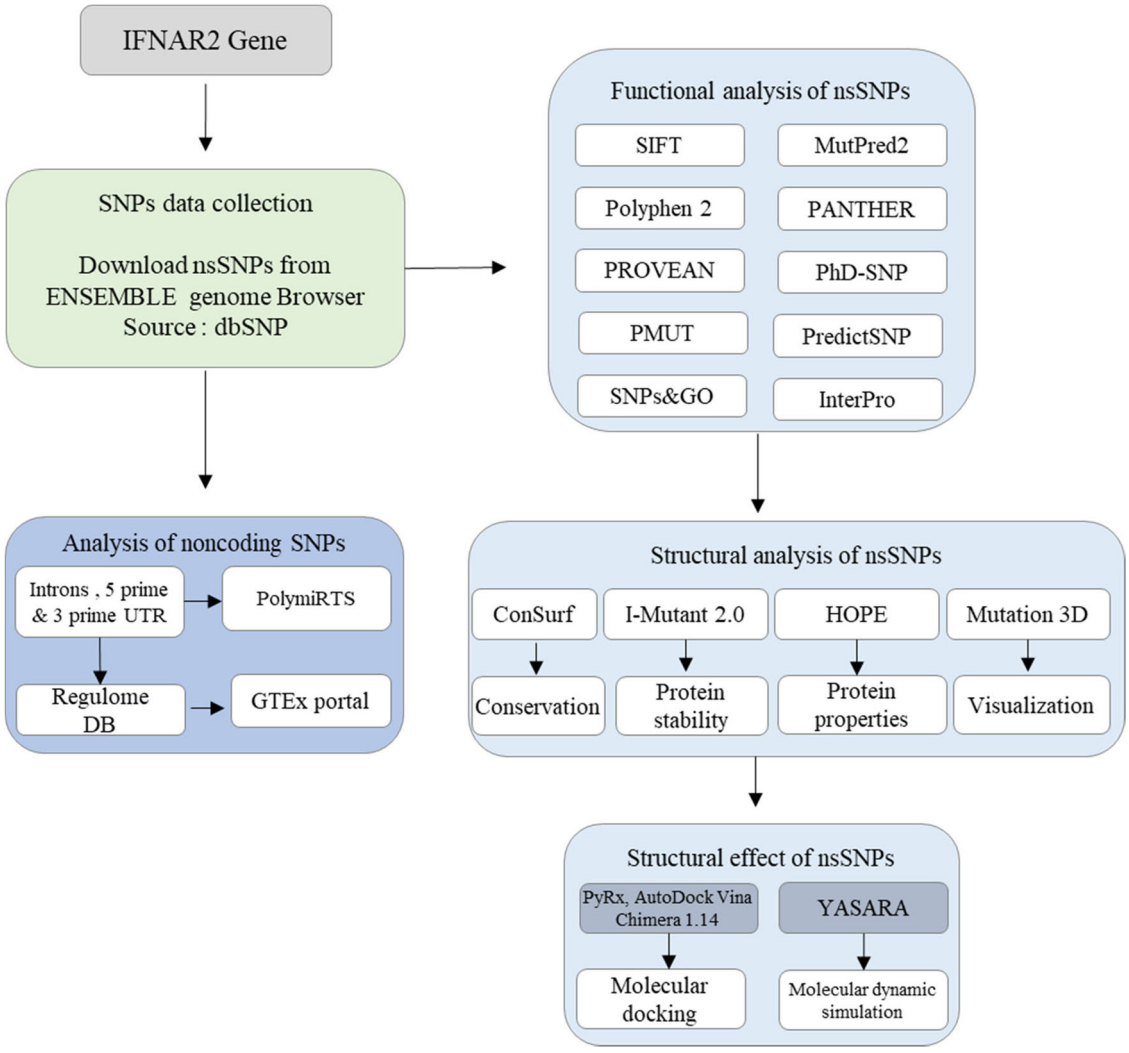


**Figure 1.** Schematic representation of *in silico* study of SNPs of human *IFNAR2* gene.

Each amino acid change and FASTA sequence of the IFNAR2 protein were required as input for the PolyPhen2 web server.

Across organisms, *PROVEAN* (Protein Variation Effect Analyzer)(Choi & Chan, 2015), which is an online tool, evaluates the functional effects of amino acid replacements or indel mutations on a protein. For human and mouse variants, PROVEAN may provide high-performance genomic and protein analysis. PROVEAN measures the score from the homologous sequence alignment for each variant and takes into consideration the score of −2.5 or lower than −2.5 to be harmful. The FASTA sequence of IFNAR2 protein and list of SNPs were entered as input into the PROVEAN Web server

To evaluate the consequence of amino acid replacements, *SNPs&GO* applies functional protein annotations and predicts the effect of SNPs based on the SVM (support vector machine) algorithm. This tool provides results from the PhD-SNP and PANTHER along with its own prediction (Capriotti et al., 2013). The input contains the 3-D protein structure or the UniProt ID, the identified SNPs/variants, and gene ontology (GO) terms. The output presents the possibility of human diseases associated with amino acid substitution.

*MutPred2* increases the priority for pathogenic amino acid substitution, predicts molecular pathways that potentially cause diseases and return the distributions of the score of pathogenicity in each genome that can be interpreted (Pejaver et al., 2020). The FASTA sequence and change in the single amino acid were entered as input on the MutPred2 web server. *p*-value cutoff was set to 0.05 as statistically significant.

*PMUT* (Piezoelectric Micromachined Ultrasonic Transducers) web tool assesses the pathology of mutations (Ferrer-Costa et al., 2005). A list of mutations or SNPs on IFNAR2 protein along with its sequence was submitted as input and we obtained their score of pathology by employing the PMUT analyst.

*PREDICT SNP* is a consensus tool that classifies SNPs based on whether they are disease-related or not. For predicting disease-related alterations, PREDICT SNP utilizes six prediction algorithms (SIFT, PhD-SNP, MAPP, SNAP, PolyPhen-1, and PolyPhen-2)(Bendl et al., 2014).

*InterPro* and *NCBI* domain prediction tools employ protein families to predict domains of protein by evaluating them functionally. The Conserved Domain Search tool in NCBI (Marchler-Bauer et al., 2015) and InterPro (Hunter et al., 2009) were used to identify the domains of the IFNAR2 protein and then SNPs were placed in different domains of it. For both domain searching tools, the input query was the FASTA amino acid sequence of the IFNAR2 protein. NCBI domain search tool used Pfam super family classification and

InterPro used different classification program such as Pfam, InterPro, PHOBIUS and Fibronectin type III superfamily to identify the domains and regions in the IFNAR2.

To test the protein stability deviation for a single nucleotide, *I-Mutant2.0* was employed as an algorithm, which uses a support vector machine. For prediction and estimation of the change in protein stability, either protein structure or protein sequence is used by I-Mutant2.0 and the corresponding Delta Delta G (DDG) values are predicted at the same time (Capriotti et al., 2005). The input was given as the protein sequence of IFNAR2 and the single amino acid replacements.

*Mutation3D* identifies alterations in amino acids in protein structures and serves as a web server (Meyer et al., 2016). Operational and non-operational variants can be detected by Mutation3D. It can be viewable in a variety of popular formats. It generates clusters of mutations from over 975,000 somatic mutations collected from the sequencing studies of 6,811 cancers.

To identify the evolutionarily conserved amino acid residues (wild type) and to detect nsSNPs in each position, we performed conservation analysis via the *ConSurf* web server (Ashkenazy et al., 2010). Based on the evolutionary relatedness between the user-submitted protein and its homologs, the ConSurf server calculates the evolutionary conservation rate of amino acid positions in that protein molecule. Consurf uses empirical Bayesian method to conduct phylogenetic analysis for calculating the conservation score. The conservation scores are divided into a discrete scale of 9 bins where bin 9 represents the most conserved positions and bin 1 represents the most variable positions. More specifically, conservation scores ranging from 1–4, 5–6, and 7–9 indicate the low, intermediate, and highly conserved amino acid, respectively. The FASTA sequence of IFNAR2 protein was entered as input and the pathogenic nsSNPs located in a particular conserved area were identified to analyze further.

## 2.3. Structural effect analysis

Structural and functional effects due to point mutations were estimated by *HOPE*. HOPE comprises data from a variety of sources including 3 D protein co-ordinate measurements using WHAT IF web services, UniProt database annotations, and DAS service predictions (Venselaar et al., 2010). Data gathered from these sources are generally classified as the impacts of mutations on three-dimensional structure and function of proteins through decision-making systems. HOPE generates a simple and straightforward report with text, graphs, and animations.

### 2.3.1. Molecular docking

The binding interaction of interferon (IFN) molecules with IFNAR2 is crucial for the functionality of various signaling cascades. Molecular docking analysis was accomplished with the *PyRx* virtual screening tool (Dallakyan & Olson, 2015) to detect the alteration in the binding pattern of IFNAR2 with IFN molecules due to the deleterious point mutations. We obtained the crystallographic structure of the IFNAR2-IFN protein complex (PDB ID: 2HYM) [ref 1] from Protein Data Bank (PDB)(Berman et al., 2000) and prepared our targeted protein using Discovery Studio72 (v4.5)(Wang et al., 2015). UCSF Chimera 1.13rc (Pettersen et al., 2004) was assigned for the preparation of the peptide sequences of IFNAR2 having deleterious nsSNPs followed by the addition of polar hydrogens as well as energy minimization using Gasteiger charges. We utilized the PDB format of the peptide sequences of IFNAR2 containing nsSNPs as ligands. Docking was performed with AutodockVina (Sanner, 1999; Trott & Olson, 2010) where we set the grid box parameters as follows: $X = 41.1918$, $Y = 52.1457$, $Z = 49.8470$. We incorporated UCSF Chimera 1.13rc (Pettersen et al., 2004) which offered the proper visualization of the binding interaction of ligands with receptor protein in the docking complex. We used UCSF Chimera 1.13rc to observe if the IFNAR2 protein has bound to the active site of IFN protein. Moreover, a deep view in the binding region of IFNAR2 and IFN was also performed by UCSF Chimera 1.13rc to identify the inter-actors (amino acid residues) participating in the binding.

### 2.3.2. Molecular dynamic (MD) simulation analysis

MD simulation was conducted using the *YASARA Dynamics* (Land & Humble, 2018) to analyze the dynamic behavior of the native and mutant IFNAR2-IFN complexes in different time scales (Krieger et al., 2012). At the very first step of the simulation, the structure of the protein-ligand complexes was cleaned along with the H-bond network optimization. Afterward, a cubic box with a periodic boundary condition was set with the grid size of ($96.9654 \times 96.9654 \times 96.9654$) Å. AMBER14 force field (Krieger et al., 2006) was adopted in the periodic cell boundary condition to simulate the system in an explicit water environment. TIP3P (transferable intermolecular interaction potential 3 points) was implemented for the addition of Sodium (Na) and Chlorine (Cl) ions for neutralizing the system. The energy minimization of the protein-ligand complexes was carried out by the steepest descent method. The cut-off radius was restricted to 8 Å to measure the short-range Coulomb and van der Waals interaction. The long-range electrostatic interactions were calculated by the PME (Particle Mesh Ewalds) method (Darden et al., 1993). This measurement was done with a physiological condition at 298 K, pH 7.4, 0.9% NaCl. For each system, MD simulation was run for 150 nanoseconds (ns) with a time step interval of 2.5 femtoseconds (fs) at 298 K. Finally, all the trajectory files were evaluated to obtain root mean square deviation (RMSD), root mean square fluctuation (RMSF), radius of gyration (Rg), solvent-accessible surface area (SASA), and hydrogen bond analysis.

## 2.4. Functional consequences of non-coding SNPs on IFNAR2 gene

An annotation of regulatory SNPs was described by *Regulome DB*. Regulome DB combines the manual interpretations of ENCODE, materials from experimental datasets, computational projections, and assign scores to variants for the

Table 1. Estimation of 13 nsSNPs with SIFT, Polyphen2, PROVEAN, MutPred2, SNPs&GO, PMUT, PhD-SNP, and PANTHER, PredictSNP.

| | | | SIFT | PolyPhen2 | POVEAN | MutPred2 | PMUT prediction | PANTHER | PhD-SNP | SNPs&GO | PredictSNP |
|---|---|---|---|---|---|---|---|---|---|---|---|
| SNP | rsID | Domain | Prediction | Prediction | Prediction | Prediction | Prediction | Prediction | Prediction | Prediction | Deleterious |
| C207F | rs1332014803 | Interfer-bind | Deleterious | Damaging | Deleterious | Disease | Disease | Disease | Disease | Disease | Deleterious |
| C85G | rs751841284 | Tissue_fac | Deleterious | Damaging | Deleterious | Disease | Disease | Disease | Disease | Disease | Deleterious |
| C85R | rs751841284 | Tissue_fac | Deleterious | Damaging | Deleterious | Disease | Disease | Disease | Disease | Disease | Deleterious |
| D94G | rs1568885326 | Tissue_fac | Deleterious | Damaging | Deleterious | Disease | Disease | Disease | Disease | Disease | Deleterious |
| I148S | rs1190725243 | Interfer-bind | Deleterious | Damaging | Deleterious | Disease | Neutral | Disease | Disease | Disease | Deleterious |
| N205I | rs758825586 | Interfer-bind | Deleterious | Damaging | Deleterious | Disease | Neutral | Disease | Disease | Disease | Deleterious |
| P136R | rs768348126 | Interfer-bind | Deleterious | Damaging | Deleterious | Disease | Disease | Disease | Disease | Disease | Deleterious |
| P202L | rs1286287301 | Interfer-bind | Deleterious | Damaging | Deleterious | Disease | Neutral | Disease | Disease | Disease | Deleterious |
| T204R | rs147496374 | Interfer-bind | Deleterious | Damaging | Deleterious | Disease | Neutral | Disease | Disease | Disease | Deleterious |
| Y106F | rs773793948 | Tissue_fac | Deleterious | Damaging | Deleterious | Disease | Disease | Neutral | Disease | Neutral | Deleterious |
| Y66C | rs772583115 | Tissue_fac | Deleterious | Damaging | Deleterious | Disease | Disease | Disease | Disease | Disease | Deleterious |
| Y70C | rs1265189745 | Tissue_fac | Deleterious | Damaging | Deleterious | Disease | Disease | Disease | Disease | Disease | Deleterious |
| P136S | rs746695388 | Interfer-bind | Deleterious | Damaging | Deleterious | Disease | Disease | Disease | Disease | Disease | Deleterious |

differentiation of SNPs from a wide pool (Boyle et al., 2012). To evaluate the outcomes of non-coding SNPs through the Regulome DB analysis, the individual variant rsIDs were used as the input in the server.

To analyze miRNA–mRNA interactions, *PolymiRTS database 3.0* integrates crosslink experimental data, ligation and hybrids sequence data (Bhattacharya et al., 2014). PolymiRTS examines the functional effects of SNPs in target sites of miRNA in IFNAR2 mRNA and miRNA seeds. To evaluate the outcomes of non-coding SNPs, the input was the individual variant ID (rsIDs) in PolymiRTS database 3.0.

In human tissues, *GTEx* (Genotype-Tissue Expression) project provides the relationship between chromosomal variations and gene expression. GTEx correlates the regulatory processing mechanisms to traits and diseases (Lonsdale et al., 2013). To evaluate the effects of non-coding SNPs, the individual variants IDs (rsIDs) were listed as input in GTEx portal. Figure 1 depicts the overall analysis for the study using different computational tools and methods. All the Web links for all *in silico* tools are presented in Table S7 (supplementary material).

## 3. Results

### 3.1. IFNAR2 SNP data retrieval

We obtained a total of 9,777 SNPs for the human *IFNAR2* gene (Transcript ID:

ENST00000342136.9) from Ensemble genome browser. The number of SNPs in different types were as follows: 1) 386 non-synonymous or missense SNPs, 2) 163 synonymous SNPs, 3) 34 frameshift SNPs, 4) 161 5prime SNPs, 5) 614 UTR SNPs, 6) 8348 Intron SNPs, 7) 50 Splice region SNPs, and 8)30 others. Different types of SNPs are provided in Figure S1.

### 3.2. Functional analysis of nsSNPS

#### 3.2.1. Determination of functionally important nsSNPs

To analyze the nsSNPs of the human *IFNAR2* gene, initially, we used SIFT and Polyphen-2. Among 386 nsSNPs, SIFT predicted 130 SNPs as deleterious which were further analyzed with Polyphen-2. Then Polyphen-2 predicted 42 nsSNPs to be probably damaging. Afterward, these 42 nsSNPs were considered for further analyses (Table S1, supplementary material and Figure 2).

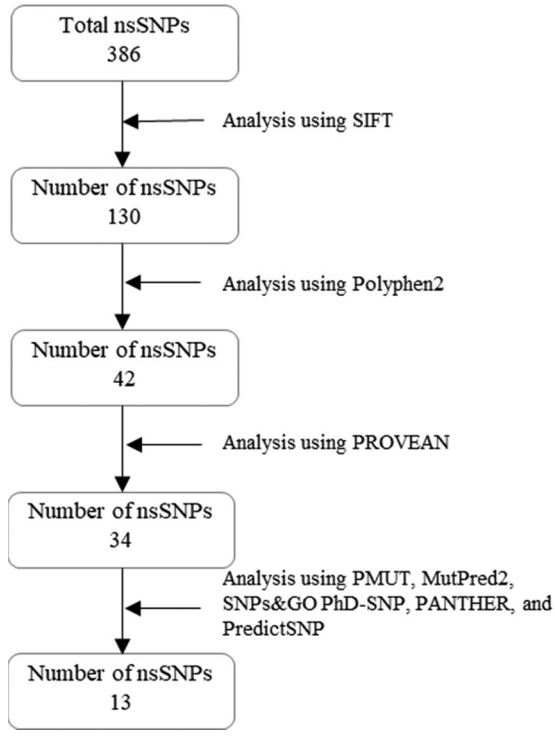


Figure 2. Schematic representation of the number of nsSNPs after subsequent analysis with In silico tools.

We used PROVEAN to predict pathogenicity for 42 SNPs which were predicted as deleterious by SIFT and Polyphen-2. Among them, 34 nsSNPs were predicted as deleterious. Moreover, the nsSNPs were evaluated through the PMUT web tool and 9 SNPs were detected as pathogenic that can cause diseases and all the others were evaluated as neutral. Additionally, *PREDICT SNP* analysis provided 39 ns SNPs as deleterious among 42 SNPs. Finally, out of 42 nsSNPs, SNPs&GO predicted 20 nsSNPs as disease associated (Table 1). Furthermore, *MutPred2* provided the structural and functional effect (i.e. gain or loss) of a specific structure or protein function and 20 nsSNPs were identified as either having loss or gain of a specific functional or structural part (Table S2, supplementary material). All prediction analysis of nsSNPs

using these tools is also provided (Figure S1, supplementary material).

We observed that there are various forms of gain or loss of protein structure or function or modified function for IFNAR2. Loss or gain of a strand, loss of disulfide linkage, altered transmembrane protein, altered ordered interface, or metal binding are notably found with significant p-value along with a high probability score. Loss of disulfide linkage is prominently found at C207F, also MutPred2 predicted P136R for the altered ordered interface, altered metal binding, or transmembrane protein.

#### 3.2.2. Determination of nsSNPs on IFNAR2 domain

The predicted domains using NCBI conserved domain search tool are 1) Tissue_fac (10-110 a.a residues) described as tissue factor domain usually binds the ligands such as Interleukins, Cytokines, or Interferons and 2) Interfer-bind (133-229 a.a) which is defined as interferon alpha/beta binding domain, according to the Pfam protein family (Figure S4, supplementary material). InterPro defined these two domains as FN3_dom (interleukins or cytokines binding) and Interferon/Interleukin_rcp_dom (interferon alpha/beta binding), respectively. InterPro homologous superfamily detected a domain of 30-238 a.a residues as FN3_sf which is also detected as Ig-like_fold (34-232 a.a), also known as Fibronectin type III superfamily domain. One region is identified as transmembrane region (12-29 a.a) and one domain named cytoplasmic domain of 269-515 a.a residues is also detected by PHOBIUS family (Figure S2, supplementary material). 13 nsSNPs, predicted as deleterious by all Insilco tools in this study were placed in the tissue_fac and interfer-bind domains (Figure 3) and presented in Figures S3 and S4 (supplementary material) after analysis by Mutation 3 D.

SIFT, PolyPhen-2, PROVEAN, MutPred2, SNPs&GO, PhD-SNP, PANTHER, and Predict SNP identified 13 nsSNPs (Figure 2) as pathogenic/deleterious which are positioned in two principal domains (tissue_fac and interfer-bind). Among them, 9 nsSNPs were detected as disease-causing by PMUT. Prioritizing the nsSNPs within the domain SNPs, 13 nsSNPs were selected for further analysis (Table 1).

Table 2. Impact of nsSNPs on the stability of IFNAR2 protein through I-mutant 2.0.

| SNP | DDG | pH | Temp | Stability |
|---|---|---|---|---|
| C85R | −0.87 | 7 | 37 | Decrease |
| Y106F | −0.11 | 7 | 37 | Decrease |
| P136R | −0.2 | 7 | 37 | Decrease |
| C207F | −0.35 | 7 | 37 | Decrease |
| C85G | −1.75 | 7 | 37 | Decrease |
| D94G | −0.93 | 7 | 37 | Decrease |
| I148S | −2.52 | 7 | 37 | Decrease |
| P136S | −0.44 | 7 | 37 | Decrease |
| N205I | 2.59 | 7 | 37 | Increase |
| P202L | −1.92 | 7 | 37 | Decrease |
| T204R | 0.19 | 7 | 37 | Increase |
| Y66C | 0.76 | 7 | 37 | Increase |
| Y70C | 0.8 | 7 | 37 | Increase |

### 3.3. Structural analysis of nsSNPs

#### 3.3.1. Evaluation of structural stability of protein

Using I-Mutant 2.0 server, 13 ns SNPs were subjected to perform the protein stability analysis at 37-degree temperature and pH 7.0. It has been predicted that protein stability is decreased due to point mutation for 9 out of 13 nsSNPs (Table 2).

#### 3.3.2. Analysis of evolutionarily conserved residues

The intensity of the evolutionary conservation for each residue of IFNAR2 was determined using ConSurf web tool and identified highly conserved structural and functional amino acid residues. ConSurf analysis predicted C85, I148, and Y106 residues as buried, structural, and highly conserved, also predicted P136, C207, D94, and P202 residues as exposed, functional, and highly conserved with the highest conservation score of 9 (Figure 4). Moreover, I148 and Y106 residues are conserved in the IFNAR2 sequence with a conservation score of 8. Thus, changes of these wild type residues to different residues due to nsSNPs were predicted as harmful for protein structure and function.

#### 3.3.3. Analysis of protein properties using hope

The structural effect of 9 nsSNPs on IFNAR2 protein was determined through Project HOPE/HOPE server. Changes in size (bigger or smaller), charge (neutral or positive or negative), and hydrophobicity were observed in the mutated residue compared to the wild type (Table S3, supplementary

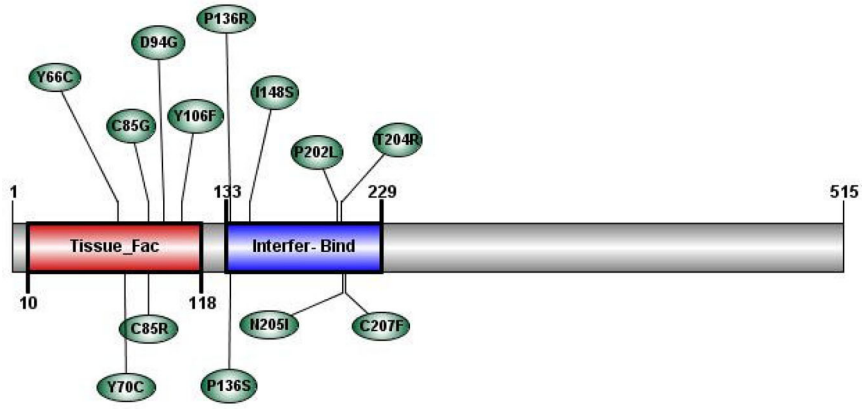


Figure 3. Predicted deleterious nsSNPs(13) are shown in two principles domain of IFNAR2.

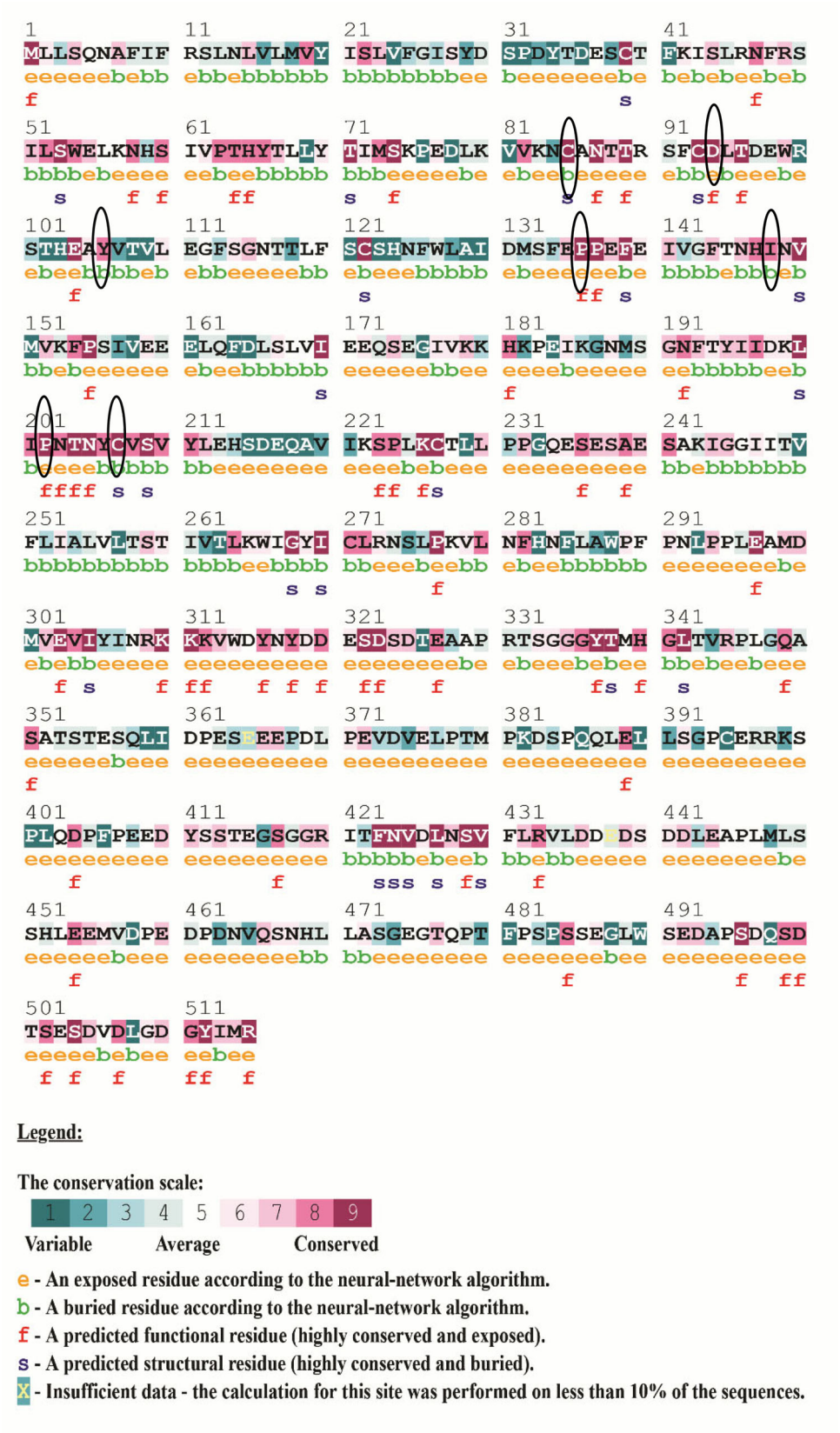


Figure 4. Evaluation of evolutionary conservation in human IFNAR2 using ConSurf; C85, D94, Y106, P136, I148, P202, C207 are highlighted in oval red box.

material). HOPE predicted that these changes would impose loss of interactions with other molecules (or domains). The loss of hydrogen bonds as a result of increased or decreased hydrophobicity enhances the disruption of correct folding of the protein. C85G, C85R, and C207F caused loss of disulfide bridge affecting the stability of IFNAR2 structure. Moreover, Glycine (G) is very flexible, which causes the loss of flexibility of the IFNAR2 structure. As Proline (P) represents special

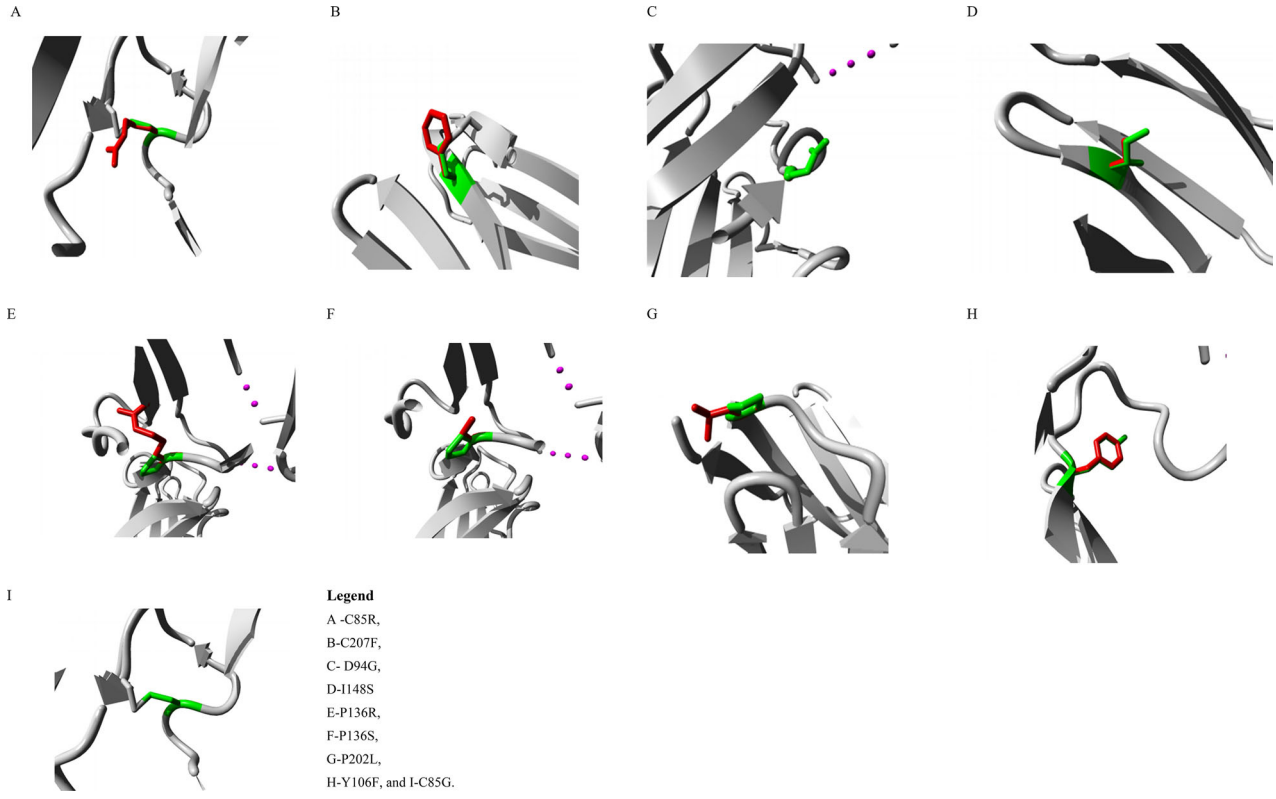


Figure 5. **A-F** represents the 9 nsSNPs predicted as deleterious by all bioinformatics tools. Visualization of the altered structure of IFNAR2 protein was done using Project HOPE. The wild type of residue is represented as green and mutated residue for each SNP is presented as red. Here, only the side chain of the residue is presented in color and the whole protein is visualized in grey color. Notably, A-C85R, E-P136R, F-P136S, D-I148S, G-P202L show that mutant residue (red colored) is much bigger than Wild type residue (green colored). In Figure A, B, and I, Cysteine is mutated to other residues and lost disulfide bridges in the structure. In case of C-D94G and I-94G, mutated residue G is not shown as it has no side chain and only green colored wild type residue is shown. All these changes in the structure possess deleterious effects in the structure and function of IFNAR2. Note: A -C85R, B-C207F, C- D94G, D-I148S, E-P136R, F-P136S, G-P202L, H-Y106F, and I-C85G.

conformation in protein structure, P136S, P136R, and P202L can cause the special conformation loss in IFNAR2 structure hampering IFNAR2 structure and function, whereas D94G may induce flexibility instead of rigidity in IFNAR2, which may also impact protein structure (Table S6, supplementary material). *3SE4* is the available 3 D-structure of IFNAR2 representing 9 nsSNPs. The images of the 9 SNPs are produced by HOPE and shown in (Figure 5).

## 3.4. Structural effect analysis of nsSNPs

### 3.4.1. Molecular docking

From the molecular docking analysis, we can determine the consequences of the point mutation over the binding interaction of IFNAR2 with its targeted IFN protein molecules. IFNAR2 binds with the active site atoms of IFN molecules, which are shown in Figure 6. Among these 9 nsSNPs, an increase in binding affinity was observed for 4 nsSNPs namely C85G, C85R, D94G, and C207F, whereas a decrease in binding affinity was found in P136S, I148S, P202L, P136R, and Y106F when compared with their wild type residues (Table 3). In the case of P136S and P136R, a remarkable reduction in binding affinity as well as hydrogen bond loss was observed after mutation. Wild type peptide sequence P136, formed 13 hydrogen bonds with the active site atoms found in the binding pocket of the IFN molecules with the binding affinity of −6.3 kcal/mol (Figure 6(A)). In case of mutant peptide sequence 136 R, only 6 hydrogen bonds were observed in the docking complex with a binding score of −5.0 kcal/mol instead of 13 hydrogen bonds found in the wild type (Figure 6(B)). On the other hand, six hydrogen bonds were found in case of P136S with a binding score of −5.2 kcal/mo. Figure 7 shows the molecular docking complexes in the active site.

### 3.4.2. Molecular Dynamic (MD) simulation analysis

MD simulation was carried out at 150 ns to observe the deviation of mutant IFNAR2-IFN complex from wild type IFNAR2-IFN complex in terms of C-$\alpha$ carbon distance between two proteins (RMSD), RMSF, Rg, SASA and H-bond in physiological conditions. RMSD values were calculated for wild type and mutant IFNAR2-IFN complexes to evaluate the extent to which mutation affects the protein complex. RMSD was calculated for all the atoms from the initial structure, which were then considered as a fundamental criterion to measure the convergence of the protein. A significant deviation in RMSD value of the IFNAR2-IFN complex was observed for the mutant P136R when compared to the native/wild type complex. RMSD analysis shows evidence that the native and mutant structures (P136R) stay close to their initial conformation till 85 ns resulting in a backbone RMSD of about 3.3 Å for mutant structure, whereas 3 Å for native. An increasing tendency in RMSD value for the mutant P136R was noticed from the 85 ns and at 105 ns mutant structure showed RMSD

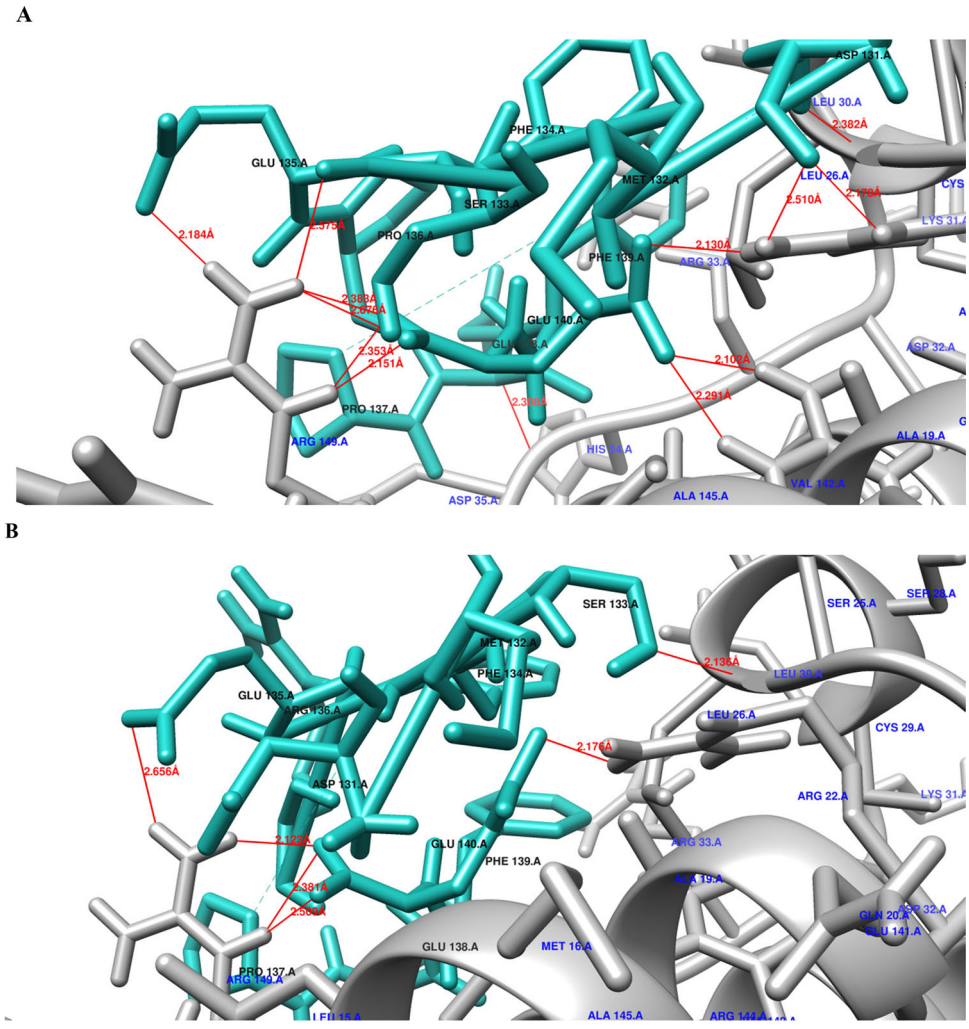


**Figure 6.** Docking complex of IFN molecules and IFNAR2 where gray color represents IFN molecules and light sea green color represents peptide sequence of IFNAR2(131aa-140aa) and hydrogen bonds are indicated by red color. (A) Wild type (P136) formed 13 hydrogen bonds with IFN molecules where Asp35 of IFN molecules binds with Glu138 of IFNAR2 with bond distance of 2.308 Å, another hydrogen bond formed between Leu26 and Asp131 with 2.382 Å distance. Arg149 formed six H bonds, among them four H bonds formed with Glu140 of IFNAR2 with distance of 2.353 Å, 2.151 Å, 2.676 Å and 2.383 Å whereas two bonds formed with Glu135 (2.184 Å) and Phe134 (2.575 Å). Arg22 formed three H bonds where 2 bonds formed with Asp131 (2.178 Å and 2.510 Å) and a single bond formed with Glu140 (2.130 Å). Arg144 formed double H bonds with Glu140 with the distance of 2.291 Å and 2.102 Å). (B) Mutant type(136R) peptide sequence formed 6 hydrogen bonds with IFN molecules. Among them, a single bond is found between Ser133 and Leu26 with the bond distance 2.136 Å. Arg149 formed four hydrogen bonds, among them, three bonds formed with Glu140 with distance of 2.123 Å,2.381 Å and 2.589 Å and another bond formed with Glu135 with the distance of 2.656 Å. Arg22 formed a single bond with Glu140 with the distance of 2.176 Å.

**Table 3.** Docking score of wild type residue and mutant residue of targeted 9 nsSNPs.

| SNP | Wild type residue | Binding affinity (kcal/mol) | Mutant residue | Binding affinity (kcal/mol) |
|---|---|---|---|---|
| C85G | C85 | −6.6 | 85G | −6.8 |
| C85R | C85 | −6.6 | 85R | −6.8 |
| D94G | D94 | −6.8 | 94G | −6.9 |
| P136S | P136 | −6.3 | 136S | −5.2 |
| I148S | I148 | −7.4 | 148S | −6.8 |
| P202L | P202 | −6.8 | 202L | −6.5 |
| C207F | C207 | −7.2 | 207F | −7.7 |
| P136R | P136 | −6.3 | 136R | −5 |
| Y106F | Y106 | −7.6 | 106F | −7.2 |

of about ∼4.471 Å where native showed 2.8 Å. The highest deviation of mutant structure (RMSD ∼11.559 Å) from the wild (RMSD ∼2.3 Å) was observed at 125 ns (Figure 8(A)). At the end of the 150 ns simulation the native structure showed RMSD of about 2.15 Å, while the mutant showed 3.86 Å. Additionally, RMSF values of mutant and native structures were determined for identifying the mutational effects to dynamic behavior of protein residues (Figure 8(B)). RMSF value of the residues of native IFNAR2 protein decreases from 7.83 Å to 1.03 Å over the entire simulation period. Conversely, an increment in residual fluctuation (7.33 Å to 12.39 Å) was observed for mutant IFNAR. The native protein showed an average of 3 Å residual fluctuation where mutant protein exhibited 10 Å. The flexibility of the residues (131-140) of native and mutant protein remains close at the initial stage of the simulation as both showed almost similar fluctuation of about 7 Å. From then, at the end of the simulation, the mutant protein was found to show greater degree of flexibility of about 12.39 Å at 140 residual positions where native showed 1.03 Å. Moreover, the highest fluctuation was observed for mutant protein (12.73 Å) when compared to native (2.8 Å) at P136R (Figure 8(B)). Furthermore, Rg analysis was carried out for measuring the compactness and rigidity of the native and mutant protein. In terms of compactness

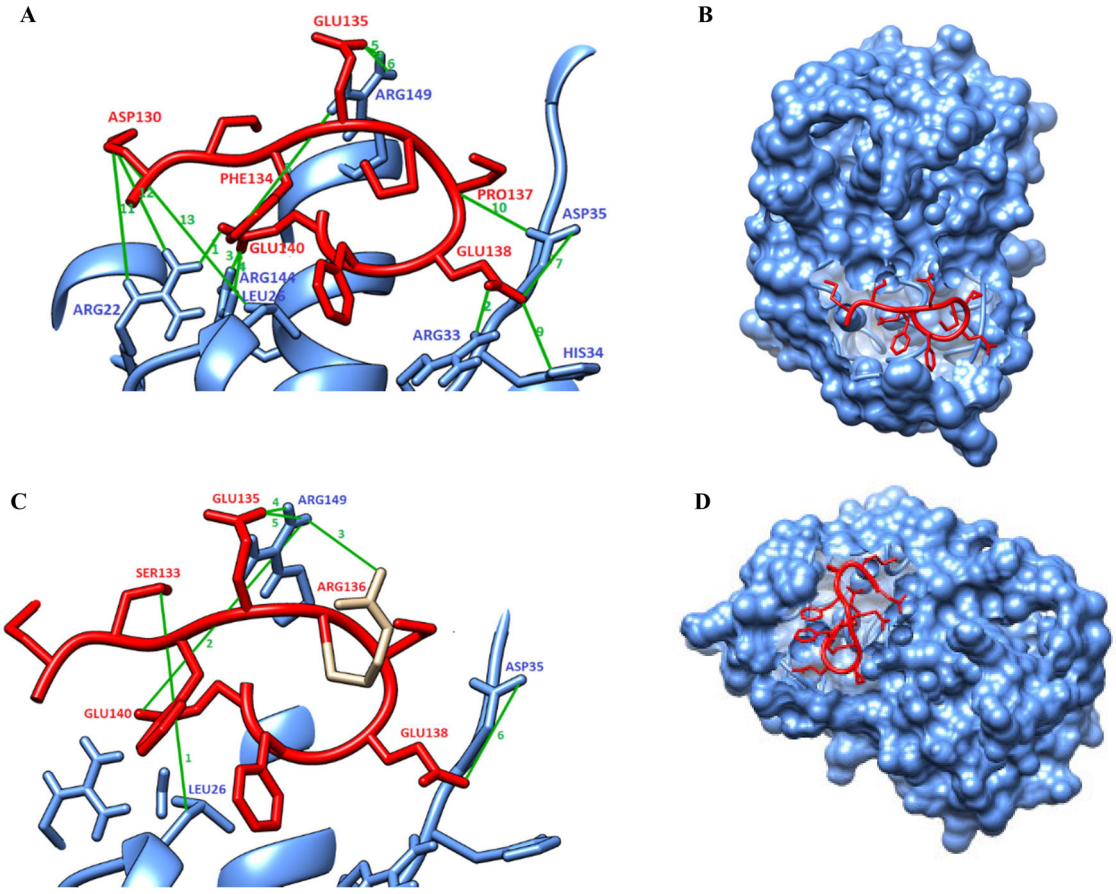


Figure 7. Molecular docking complexes of IFNAR2-IFN showing active site of IFN molecule with IFNAR2 wild type or mutant peptide. A and C represent the close view of active sites for wild type -IFN complex and mutant(136R)-IFN complex, respectively. B and D show the surface representation of the wild type-IFN complex and mutant136R peptide - IFN complex, respectively.

and rigidity the native and mutant structures remained close till 94 ns resulting in a backbone Rg of about 16.94 Å for mutant structure whereas 16.38 Å for native (Figure 8(C)). Rg analysis showed that the value of Rg significantly deviated from 94 ns (16.942 Å) to 144 ns (17.184 Å) of 150 ns MD simulation when compared to native (Figure 7(C)). Most prominent flexibility in the backbone of the mutant protein was noticed at 124 ns with Rg value of 19.32 Å. On the contrary, at 124 ns native protein showed 16.96 Å of Rg value. Besides, we conducted SASA analysis of the native and mutant complex to determine the expansion of the protein surface area. SASA analysis indicated that mutant P136R showed less average SASA value (9901.682 $Å^2$) than the native (9997.871 $Å^2$) (Figure 8(D)). The lowest SASA value of 9325.64 $Å^2$ at 28 ns was observed for mutant protein, whereas native showed 9961.70 $Å^2$ at 28 ns. Additionally, the highest SASA value for mutant protein was noticed at 118 ns of 10437.07 $Å^2$, whereas native showed 10772.74 $Å^2$. Higher degree of deviation in expansion of protein surface area was noticed at the end of 150 ns simulation where SASA value was 9624.25 $Å^2$ for mutant protein and 10755.38 $Å^2$ for native one (Figure 8(E)). H-bond analysis demonstrated that the native protein had a maximum number of 159 hydrogen bonds at 97 ns, whereas 144 hydrogen bonds were observed for mutant-IFN complex. Most prominent loss in hydrogen bond was observed from 108 ns to 130 ns for mutant protein. In this time frame the native/wild type showed an average of 140 hydrogen bonds, whereas the mutant showed 127 hydrogen bonds. At the end of the 150 ns, 132 hydrogen bonds were found for the mutant complex and 140 for the wild type/native complex.

### 3.5. Non-Coding SNPs analysis of IFNAR2 protein using RegulomeDB

Noncoding SNPs of the *IFNAR2* gene for transcript ID ENST00000342136.9 were obtained from the Ensemble genome browser using the NCBI dbSNP source. 109 non-coding SNPs that include 5 prime UTR, 3 prime UTR variants, and introns, were obtained considering the Global MAF range of 0.034-0.5. Later RegulomeDB analysis was performed for all SNPs and the filtering process was done using ranking criteria proposed in RegulomeDB website resulting in 21 SNPs (Table S4, supplementary material). Out of 21 SNPs, there are 19 intron variants, one 3 prime UTR and one 5 prime UTR variants.

#### 3.5.1. Polymirts analysis of noncoding SNPs

All the non-coding SNPs (109) identified from the Ensemble genome browser were analyzed by PolymiRTs web server. Primarily, 27 SNPs were found with miRbase ID and miRNA site. Later, These SNPs were evaluated based on their functional class (C, D) and conservation score (10-3). Finally, 10

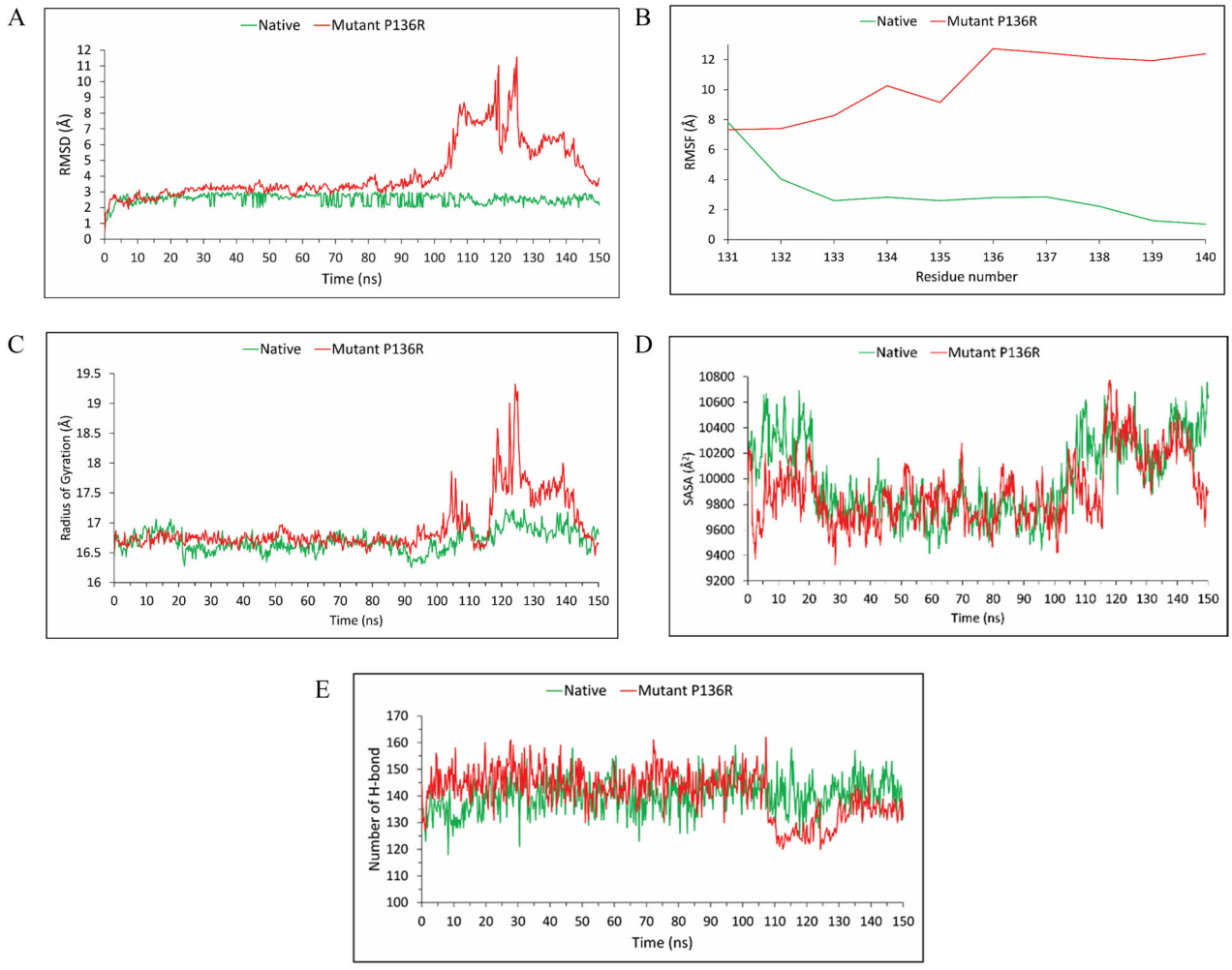


**Figure 8.** (A) RMSD analysis of Cα atoms of wild type and mutant IFNAR2-IFN protein complex's structure at 150 ns. (B) RMSF analysis of the residues of the wild type and mutant IFNAR2 protein over the 150 ns simulation. (C) Rg analysis of the wild type and mutant IFNAR2-IFN protein complex's backbone over the 150 ns. (D) SASA analysis of the wild type and mutant IFNAR2-IFN protein complex over the 150 ns. (E) Hydrogen bond analysis of the wild type and mutant IFNAR2-IFN complex over 150 ns.

(ten) 3 prime -UTR SNPs were obtained for IFNAR2 gene (Table S5, supplementary material). One SNP was observed to be associated with Crohn's disease and this association has been published in an earlier study[50].

### 3.5.2. Finding eQTLs using GTEx portal

To identify the single tissue eQTLs and sQTLs, 21 filtered RegulomeDB analyses were investigated in further detail in the GTEx portal. A total of 137 eQTLs were obtained for 21 SNPs and 270 sQTLs also were retrieved for 15 SNPs expressing the *IFNAR2* gene significantly. eQTLs and sQTLs were found in different types of tissues: Adipose, Brain, Lung, Esophagus-Mucosa, Heart-Atrial Appendage/left ventricle, Skeletal Muscle, Pancreas, Skin, Stomach, Cultured fibroblasts cells, Nerve-Tibia, and whole blood (Figure 9(A)). sQTLs are also presented in other tissues: Liver, Prostate, Spleen, Thyroid, and Colon. Notable findings are lung tissue eQTLs and sQTLs expressing SNPs in *IFNAR2*. There are 14 sQTLs and 5 eQTLs for lung tissues (Table 4). sQTLs and eQTLs SNPs are significantly observed in adipose tissue, whole blood, and skin tissue (Figure 9(B)). Violin plots of 14 sQTLs and 5 single tissue eQTLs generated from GTEx analysis are also provided (Figures S5 and S6, supplementary material**)**.

## 4. Discussion

COVID-19 disease is a global public health danger throughout the world caused by SARS-CoV-2 virus. As mentioned earlier, nsSNPs or variants of the *IFNAR2* gene were found to be associated with traits, disease, or infection susceptibility (Pairo-Castineira et al., 2021)(Frodsham et al., 2006), i.e. COVID-19 severe illness, we executed a thorough categorization of the SNPs of *IFNAR2* gene by applying a wide variety of *in silico* tools and identified the harmful/pathogenic effects of 9 nsSNPs on IFNAR2 protein structure, function, and stability. We also found several *in silico* studies that characterized nsSNPs in different genes (Abdul Samad et al., 2016; Chakraborty et al., 2018; Lopez et al., 2021; Sen Gupta et al., 2020). *IFNAR2* gene encodes for IFNAR2 protein that forms dimeric complex with Interferon alpha/beta receptor protein, IFNAR1(Novick et al., 1994), has a crucial role in the Type I interferon signaling pathway that is involved in

immune response at the first line of protection against COVID-19 disease (Lee & Shin, 2020). In response to any foreign particle, activation of phosphorylation of cellular proteins is required to respond to combat the unfavorable condition of the human body and stimulates the release of numerous essential elements for early host response. IFNAR2 has a high binding affinity for ligands, thus early responding Interferons (IFNs) bind to IFNAR2, subsequently IFNAR1 and then other members in the type1 pathway are activated to respond to viral infection (Sadler & Williams, 2008; Zou et al., 2016). As the IFNAR2 protein/receptor is an essential component in that pathway, we are interested to explore the *IFNAR2* gene in this study and have decided to characterize the SNPs which may be responsible for severe illness in COVID-19 disease. Therefore, we intended to employ several *in silico* tools to assess the missense and noncoding SNPs. A wide range of tools have been implemented to make higher accuracy predictions on the functional impact of the nsSNPs. Most methods are constructed based on sequence or structural characteristics, while tools such as Polyphen 2.0 implement both 3 D-structure and sequence and thereby give more robust predictions than those based only on sequence information (Rodriguez-Casado, 2012). Current trend prefers using a variety of tools to categorize variants as detrimental or benign rather than a single tool (Alonso-Gonzalez et al., 2018). SNPs were categorized by SIFT and PROVEAN based on alignment data. Incorporating structural data, the PolyPhen and SNPs&GO applications reinforced the prediction results.

In our study, at the beginning, 42 nsSNPs were predicted as deleterious by SIFT and PolyPhen2 and 13 nsSNPs were predicted as pathogenic out of 42 which were examined sequentially by rest of the tools (Figure 2). Then, among these 13 SNPs, I-mutant 2.0 predicted 9 nsSNPs to reduce the stability of protein. These identified 9 nsSNPs are D94G, C207F, P136R, C85G, C85R, P136S, Y106F, I 148S, P202L in IFNAR2 protein that may cause destabilization of IFNAR2 in SARS-CoV-2 infected people. Mutation 3 D analysis shows two domains of IFNAR2: (1) tissue_fac, (2) Interfer-bind domain containing all 9 nsSNPs. Interfer-bind is the interferon binding domain which is essential for interferon bindings such as type I interferon alpha or beta, interaction with cytokines and protein kinases (JAK1). JAK1 phosphorylates STAT1 which forms dimer with STAT2 involving in transcriptional activation of target genes to respond to infectious agents like coronavirus (Zou et al., 2016). These 9 nsSNPs may have a negative impact on IFNAR2 production leading to severe illness in COVID-19 disease. In addition, the structural effect analysis had been performed through 1) HOPE, 2) molecular docking of protein-protein interactions, and 3) molecular dynamic simulation of IFNAR2-IFN complex.

HOPE analysis indicated the loss of interactions with ligand (IFNs), other domains or other molecules in other domains for 9 ns SNPs due to change in amino acid properties resulting in altered function of protein IFNAR2. Spatiotemporal dynamics of protein-protein interactions are affected by protein mass and charge variation (Peleg et al., 2014; Xu et al., 2013)). Notably, P136R/S, P202L presents special essential conformation loss due to change of proline to arginine or serine or leucine and C207F, C85G/R possess loss of disulfide bridge due to changes from cysteine to other

**Table 4.** sQTLs and eQTLs in lung tissue for non-coding SNPs.

| QTLs | Gene symbol | SNP id | P-value | NES | Tissue |
|---|---|---|---|---|---|
| eQTLs | *IFNAR2* | rs13052526 | 2.1E-06 | 0.16 | Lung |
| | *IFNAR2* | rs2250226 | 5.1E-06 | −0.12 | Lung |
| | *IFNAR2* | rs2252650 | 0.000033 | 0.11 | Lung |
| | *IFNAR2* | rs2300371 | 0.000081 | −0.11 | Lung |
| | *IFNAR2* | rs6517156 | 5.3E-06 | −0.12 | Lung |
| sQTLs | *IFNAR2* | rs11088247 | 8.8E-24 | 0.39 | Lung |
| | *IFNAR2* | rs1131964 | 7.4E-07 | 0.18 | Lung |
| | *IFNAR2* | rs12482193 | 2.3E-29 | 0.44 | Lung |
| | *IFNAR2* | rs2248202 | 1.5E-06 | 0.19 | Lung |
| | *IFNAR2* | rs2248420 | 1.4E-28 | 0.44 | Lung |
| | *IFNAR2* | rs2250226 | 4E-22 | 0.36 | Lung |
| | *IFNAR2* | rs2252650 | 1.2E-26 | −0.4 | Lung |
| | *IFNAR2* | rs2284550 | 1.2E-10 | −0.23 | Lung |
| | *IFNAR2* | rs2300371 | 1.5E-29 | 0.44 | Lung |
| | *IFNAR2* | rs2834158 | 1.8E-24 | −0.39 | Lung |
| | *IFNAR2* | rs2834164 | 1.2E-10 | −0.23 | Lung |
| | *IFNAR2* | rs2834165 | 8.7E-11 | −0.23 | Lung |
| | *IFNAR2* | rs6517153 | 8.8E-24 | 0.39 | Lung |
| | *IFNAR2* | rs6517156 | 4.1E-24 | 0.39 | Lung |

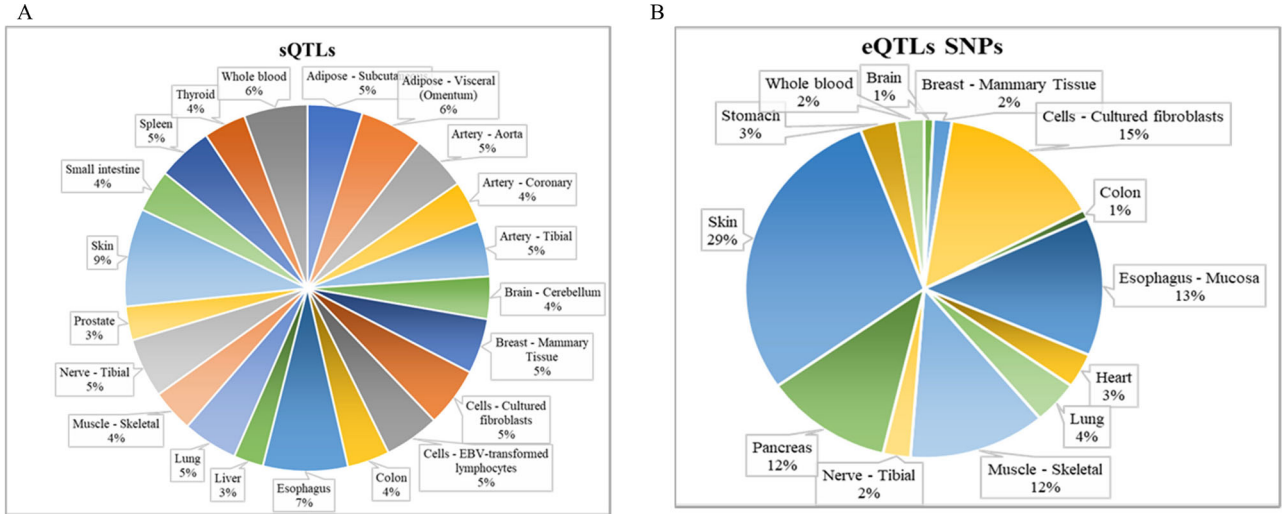


**Figure 9.** (A) distribution of sQTLs, and (**B**) eQTLs in different tissues for non-coding SNPs of IFNAR2 gene.

residues. P136R and C85R introduces charges that can result in a rejection between the mutant and neighboring residues (Peleg et al., 2014). The variants thus distort the linkage with the surrounding residues to disturb normal biological processes. These changes lead to loss of thermodynamic stability, abnormal folding and protein aggregation (Rodriguez-Casado, 2012) (Figure 5 and Table S6, supplementary material). All these 9 residues are conserved and located in the interferon binding domain (functional) causing the disturbance or hindrance in protein function (Figure 4). After primary validation of these 9 nsSNPs which were predicted as pathogenic through all tools, we performed molecular docking of IFNAR2 and IFN complex for further verification. 5 ns SNPs (P136S, I148S, P202L, P136R and Y106F) showed decrease in binding affinity as binding energy becomes less negative compared to wild type residues in IFNAR2. The remarkable decrease in binding affinity (BA) for P136R and P136S was resulted from loss of hydrogen bonds (13 to 6) in the docked complexes of IFNAR2 and IFN. Studies for drug design (Ghosh et al., 2020a, 2020b) performed Molecular Docking using Auto dock Vina and found high binding affinity of ligands (highly negative BA score) for protein that states highly stable binding of ligand -protein complex. In the case of our study, to identify the significant mutations or nsSNPs, it was required to examine low binding affinity (less negative or positive BA score compare to wild type) that can destabilize the mutant IFNAR2-IFN complex. (Hossain et al., 2020) performed the similar type of analysis using AutoDock Vina and Pyryx tools to find out the significant ns SNPs. In another study, mutant protein; 234 R- LATS2 has reduced binding affinity score (∼21.0 Kcal/mol) compare to wild type (-11 Kcal/mol) and had impact on the stability of the merlin protein (Havranek & Islam, 2020). Therefore, loss of hydrogen bonds and binding affinity reductions has a direct effect on the stability of the IFNAR2-IFN complex by lowering the probability of ligand binding with the receptor. Thus, our results verified the pathogenicity of nsSNPs on protein function and structure leading to deficient activity of the receptor in COVID-19 disease. Moreover, high binding affinity score of mutant-protein complex explains the higher stability than wild type and these nsSNPs of IFNAR2 protein can be used to find out the effective drugs to treat COVID-19 severely ill patients.

The static postures of the most preferred molecular conformation are provided by molecular docking in the binding pocket of a protein to create a stable complex but cannot show the other important features that contribute to a protein stability involving residue flexibility and secondary construction elements (Purohit, 2014). Conformational changes resulting from a protein's dynamic behavior could affect its actual biology (Bhardwaj & Purohit, 2020). MD simulations could visualize the actual motion and structural disruption of a protein in its biological environment. Though we have obtained 5 ns SNPs with lower binding affinity for IFN, we performed MD simulations for one nsSNP (P136R) as this ns SNP was predicted as highly pathogenic by all implemented Insilco tools together with significant structural effect predicted by I-mutant 2.0 and Project Hope. Molecular Dynamics simulations showed the decreased stability of P136R mutant-IFNAR2 complex at normal physiological condition in the human body compared to wild type protein. Four different types of analysis: RMSD, RMSF, Rg, SASA showed significant deviation in case of mutant IFNAR2-IFN complex compared to wildtype IFNAR2-IFN complex. Distinctively, increased *RMSD* value for P136R mutant-IFN complex structure at 105-125 ns, explains the separation or destruction of the bound complex. The lower the RMSD, the higher is the stability of the protein. However, the constant RMSD value of the wild type IFNAR2-IFN complex shows the intactness of the complex, indicating that this complex is stable (Figure 8(A)). This analysis concludes that the substitution of Proline with Arginine at 136 positions in IFNAR2 protein prevalently deviates its structure from the native conformation which could affect the binding affinity of the protein with IFN. As a result, the IFNAR2-IFN complex may not be able to play its normal functionality(Islam et al., 2019)).) Results from *RMSF a*nalysis revealed that due to the mutation (P136R) at position 136 of the IFNAR2 protein, higher degree of residual fluctuation was observed at positions 131-140 which made that region more flexible than wild type leading to lose of binding of IFNAR2 with IFN (Figure 8(B)). Rg value deviation for mutant complex to native complex, may create the IFNAR2-IFN complex less compact than wild type which may increase the flexibility of the complex, affecting the binding of IFNAR2 to IFN (Figure 8(C)). (Figure 8(D)) showed the *SASA* findings and entailed that the average SASA value of mutant protein always remained less than the wild type suggesting that the mutant-IFN protein complex's surface area was not as expand as the IFNAR2- wild type-IFN protein complex for the effective binding of IFNAR2 to IFN. The reason behind the deviation in RMSD, RMSF, Rg and SASA value of native and mutant protein was further validated by hydrogen bond analysis. Decreased number of *H-bonds* for mutant complex (Figure 8(E)) supports the RMSD, RMSF, Rg and SASA findings and interprets that the mutant-IFN complex was damaged after a certain time directing towards unstable condition of the complex. All these findings conclude that the P136R mutation may have a deleterious effect on the stability of IFNAR2-IFN complex and also proves the damaging effect of P136R in protein function by hampering the binding of IFN to the IFNAR2 in response to SARS-CoV-2 infection. Similar results were obtained from RMSD, RMSF, Rg, H-bond and SASA analysis in many prior studies for different mutant protein-ligand complex for respective goal (Abdul Samad et al., 2016; Chakraborty et al., 2018; Islam et al., 2019; Dash et al., 2020; Ghosh et al., 2020b, 2020a; Havranek & Islam, 2020; Owji et al., 2020; Choudhury et al., 2021; Lopez et al., 2021; Sen Gupta et al., 2020).

miRNA binds to mRNA of *IFNAR2* to regulate the production of IFNAR2 protein by causing translation suppression and mRNA damage. 3 prime UTR SNPs in IFNAR2 creates or disrupts target sites in mRNA affecting the interaction of miRNA-mRNA and subsequently may result in miRNA-mediated abnormal IFNAR2 repression (Moszyńska et al., 2017) and affect normal IFNAR2 receptor production leading

to reduced normal IFNAR2 level. Thus, this finding may have a negative effect on overall immune response in the human body. Hence, this understanding explains lower immune response in COVID-19 in severely ill individuals too.

Characterization of the variation of gene expression levels due to variants (SNPs) is attained through GTEx portal with large sample size along with a wide range of tissues of the human body (Aguet et al., 2017).In this study, GTEx portal analysis provided 270 sQTLs and 137 eQTLs for one 3 prime UTR, one 5 prime UTR and remaining intron SNPs of *IFNAR2* gene in many tissues in human (Figure 9(A) and (B)). QTLs play an important role in disease phenotypes or differing expression of genes either by affecting spicing mechanism through sQTLs or by affecting the expression levels of IFNAR2 through eQTLs (Westra & Franke, 2014). sQTLs are present in introns having an essential role in numerous splicing incidents (Garrido-Martín et al., 2021). One of the two ways to regulate splicing events is the direct alteration of splicing configurations by variants in sQTLs. Throughout the populations, gene expression of a particular gene varies due to the variation in genetic architecture; SNPs in eQTLs (Mogil et al., 2018) reflecting the epidemiological record which represents in various populations and has been demonstrated to associate with new traits (Pala et al., 2017). Intron SNPs in sQTLs of *IFNAR2* can negatively regulate the splice events leading to hinder the translation process to produce IFNAR2 receptor associating with the lower level of the protein in lung, adipose tissue, skin, heart, and pancreas in various individuals. Thus, lower immune response in adipose tissue, skin and lung in COVID-19 patients resulting in severe illness in those patients. Similarly, the eQTLs SNPs in different individuals cause new traits such as high expression of the *IFNAR2* gene with several regulatory SNPs ending up with lower production of IFNAR2. This causes lower receptor level for IFN binding in response to foreign particles in lung, adipose tissue, skin, heart, and pancreas for severely ill COVID-19 patients.

## 5. Conclusion

In this study, we employed various *in silico* tools and found 9 pathogenic nsSNPs which are unreported in UniProt database, can modify the structure and function of IFNAR2 protein. Further, among 9 ns SNPs, two of them: P136R and P136S were observed to be highly deleterious by molecular docking through determining the reduced binding affinity for IFN molecules. Later our Molecular dynamic simulation presented a significant deviation in functional domain of IFNAR2 with mutant structure compared to wild type IFNAR2 complexed with IFN molecule. These changes can interrupt the native conformation of IFNAR2 leading to reduce the functionality in response to coronavirus infection. The non-coding SNP analysis reveals an interference with miRNA binding site that may disturb the expression of IFNAR2 protein. GTEx assessment found the single tissue eQTLs and sQTLs SNPs which show the hindrance of expression or post transcriptional modification of *IFNAR2* gene in lung tissue resulting in reduced production of the receptor for severely ill patients in COVID-19. The findings of this study will help the researchers and medical practitioners to detect deleterious SNPs associated with the severity of the illness in different individual patients in COVID-19, consequently, assist to develop an effective drug against the infection in future. Hence, clinical-trial-based research is necessary comprehensively on a substantial population to finalize these SNPs along with experimental validation through mutational studies.

## Acknowledgements

The authors acknowledge sincere support provided by *Md. Shahadat Hossain* and the Lab at Department of Biotechnology and Genetic Engineering, Noakhali Science and Technology University, Noakhali, Bangladesh.

## Disclosure statement

No potential conflict of interest was reported by the author(s).

## ORCID

*Shamima Akter* http://orcid.org/0000-0001-9119-5197
*Md Sajedul Islam* http://orcid.org/0000-0002-3649-8037

## Author contributions

S.A, and M.S.I conceived and designed the study. S.A. collected the data and analyzed all the SNPs using in silico tools. A.S.R performed the Molecular Docking and M.I.Q.T performed the Molecular dynamics simulation. S.A, M.S.I, A.S.R, and M.I.Q.T discussed and interpreted the results. S.A drafted the manuscript. S.A, M.S.I, A.S.R, and M.I.Q.T revised the manuscript. All authors read and agreed to the submitted version of the manuscript.

## References

Abdul Samad, F., Suliman, B. A., Basha, S. H., Manivasagam, T., & Essa, M. M. (2016). A comprehensive In Silico analysis on the structural and functional impact of SNPs in the congenital heart defects associated with NKX2-5 gene – a molecular dynamic simulation approach. *PLoS One*, *11*(5), e0153999–16. https://doi.org/10.1371/journal.pone.0153999

Adzhubei, I. A., Schmidt, S., Peshkin, L., Ramensky, V. E., Gerasimova, A., Bork, P., Kondrashov, A. S., & Sunyaev, S. R. (2010). A method and server for predicting damaging missense mutations. *Nature Methods*, *7*(4), 248–249. https://doi.org/10.1038/nmeth0410-248

Aguet, F., Brown, A. A., Castel, S. E., Davis, J. R., He, Y., Jo, B., Mohammadi, P., Park, Y. S., Parsana, P., Segrè, A. V., Strober, B. J., Zappala, Z., Cummings, B. B., Gelfand, E. T., Hadley, K., Huang, K. H., Lek, M., Li, X., Nedzel, J. L., … Zhu, J. (2017). Genetic effects on gene expression across human tissues. *Nature*, *550*(7675), 204–213. https://doi.org/10.1038/nature24277

Akter, S., Hossain, S., Hosen, M. I., & Shekhar, H. U. (2021). Comprehensive Characterization of the Coding and Non-coding Single Nucleotide Polymorphisms in the Tumor Protein p63 (TP63) Gene Using In. *Scientific Reports*, *63*, 1–13.

Alonso-Gonzalez, A., Rodriguez-Fontenla, C., & Carracedo, A. (2018). De novo mutations (DNMs) in autism spectrum disorder (ASD): Pathway and network analysis. *Frontiers in Genetics*, *9*(SEP), 406. https://doi.org/10.3389/fgene.2018.00406

Arunachalam, P. S., Wimmers, F., Mok, C. K. P., Perera, R. A. P. M., Scott, M., Hagan, T., Sigal, N., Feng, Y., Bristow, L., Tak-Yin Tsang, O., Wagh, D., Coller, J., Pellegrini, K. L., Kazmin, D., Alaaeddine, G., Leung, W. S., Chan, J. M. C., Chik, T. S. H., Choi, C. Y. C., … Pulendran, B. (2020). Systems biological assessment of immunity to mild versus severe

COVID-19 infection in humans. *Science (New York, N.Y.)*, *369*(6508), 1210–1220. https://doi.org/10.1126/science.abc6261

Ashkenazy, H., Erez, E., Martz, E., Pupko, T., & Ben-Tal, N. (2010). ConSurf 2010: Calculating evolutionary conservation in sequence and structure of proteins and nucleic acids. *Nucleic Acids Research*, *38*(Web Server issue), W529–W533. https://doi.org/10.1093/nar/gkq399

Bastard, P., Rosen, L. B., Zhang, Q., Michailidis, E., Hoffmann, H.-H., Zhang, Y., Dorgham, K., Philippot, Q., Rosain, J., Béziat, V., Manry, J., Shaw, E., Haljasmägi, L., Peterson, P., Lorenzo, L., Bizien, L., Trouillet-Assant, S., Dobbs, K., de Jesus, A. A., … Casanova, J.-L, HGID Lab§. (2020). Autoantibodies against type I IFNs in patients with life-threatening COVID-19. *Science*, *370*(6515), eabd4585. https://doi.org/10.1126/science.abd4585

Beck, D. B., & Aksentijevich, I. (2020). Susceptibility to severe COVID-19. *Science (New York, N.Y.)*, *370*(6515), 404–405. https://doi.org/10.1126/science.abe7591

Bendl, J., Stourac, J., Salanda, O., Pavelka, A., Wieben, E. D., Zendulka, J., Brezovsky, J., & Damborsky, J. (2014). PredictSNP: Robust and accurate consensus classifier for prediction of disease-related mutations. *PLoS Computational Biology*, *10*(1), e1003440. https://doi.org/10.1371/journal.pcbi.1003440

Berman, H. M., Westbrook, J., Feng, Z., Gilliland, G., Bhat, T. N., Weissig, H., Shindyalov, I. N., & Bourne, P. E. (2000). The protein data bank. *Nucleic Acids Research*, *28*(1), 235–242. https://doi.org/10.1093/nar/28.1.235

Bhardwaj, V. K., & Purohit, R. (2020). A new insight into protein-protein interactions and the effect of conformational alterations in PCNA. *International Journal of Biological Macromolecules*, *148*, 999–1009. https://doi.org/10.1016/j.ijbiomac.2020.01.212

Bhardwaj, V. K., Singh, R., Das, P., & Purohit, R. (2021). Evaluation of acridinedione analogs as potential SARS-CoV-2 main protease inhibitors and their comparison with repurposed anti-viral drugs. *Computers in Biology and Medicine*, *128*, 104117. https://doi.org/10.1016/j.compbiomed.2020.104117

Bhattacharya, A., Ziebarth, J. D., & Cui, Y. (2014). PolymiRTS Database 3.0: Linking polymorphisms in microRNAs and their target sites with human diseases and biological pathways. *Nucleic Acids Research*, *42*(Database issue), D86–D91. https://doi.org/10.1093/nar/gkt1028

Boyle, A. P., Hong, E. L., Hariharan, M., Cheng, Y., Schaub, M. A., Kasowski, M., Karczewski, K. J., Park, J., Hitz, B. C., Weng, S., Cherry, J. M., & Snyder, M. (2012). Annotation of functional variation in personal genomes using RegulomeDB. *Genome Research*, *22*(9), 1790–1797. https://doi.org/10.1101/gr.137323.112

Capriotti, E., Calabrese, R., Fariselli, P., Martelli, P. L., Altman, R. B., & Casadio, R. (2013). WS-SNPs&GO: A web server for predicting the deleterious effect of human protein variants using functional annotation. *BMC Genomics.*, *14*(Suppl 3), S6–S7. https://doi.org/10.1186/1471-2164-14-S3-S6

Capriotti, E., Fariselli, P., & Casadio, R. (2005). I-Mutant2.0: Predicting stability changes upon mutation from the protein sequence or structure. *Nucleic Acids Research*, *33*(Web Server issue), W306–W310. https://doi.org/10.1093/nar/gki375

Cargill, M., Altshuler, D., Ireland, J., Sklar, P., Ardlie, K., Patil, N., Shaw, N., Lane, C. R., Lim, E. P., Kalyanaraman, N., Nemesh, J., Ziaugra, L., Friedland, L., Rolfe, A., Warrington, J., Lipshutz, R., Daley, G. Q., & Lander, E. S. (1999). Characterization of single-nucleotide polymorphisms in coding regions of human genes [published erratum appears in. *Nature Genetics*, *22*(3), 231–238. 1999 Nov;*Nature Genetics*, (3)231. 238. https://doi.org/10.1038/10290

Chakraborty, R., Gupta, H., Rahman, R., & Hasija, Y. (2018). In silico analysis of nsSNPs in ABCB1 gene affecting breast cancer associated protein P-glycoprotein (P-gp). *Computational Biology and Chemistry*, *77*, 430–441. https://doi.org/10.1016/j.compbiolchem.2018.08.004

Chen, N., Zhou, M., Dong, X., Qu, J., Gong, F., Han, Y., Qiu, Y., Wang, J., Liu, Y., Wei, Y., Xia, J., Yu, T., Zhang, X., & Zhang, L. (2020). Epidemiological and clinical characteristics of 99 cases of 2019 novel coronavirus pneumonia in Wuhan, China: A descriptive study. *The Lancet*, *395*(10223), 507–513. https://doi.org/10.1016/S0140-6736(20)30211-7

Choi, Y., & Chan, A. P. (2015). PROVEAN web server: A tool to predict the functional effect of amino acid substitutions and indels. *Bioinformatics (Oxford, England)*, *31*(16), 2745–2747. https://doi.org/10.1093/bioinformatics/btv195

Choudhury, A., Mohammad, T., Samarth, N., Hussain, A., Rehman, M. T., Islam, A., Alajmi, M. F., Singh, S., & Hassan, M. I. (2021). Structural genomics approach to investigate deleterious impact of nsSNPs in conserved telomere maintenance component 1. *Scientific Reports*, *11*(1), 1–13. https://doi.org/10.1038/s41598-021-89450-7

Clohisey, S., & Baillie, J. K. (2019). Host susceptibility to severe influenza A virus infection. *Critical Care*, *23*(1), 1–10. https://doi.org/10.1186/s13054-019-2566-7

Czarny, P., Wigner, P., Strycharz, J., Watala, C., Swiderska, E., Synowiec, E., Galecki, P., Talarowska, M., Szemraj, J., Su, K. P., & Sliwinski, T. (2018). Single-nucleotide polymorphisms of uracil-processing genes affect the occurrence and the onset of recurrent depressive disorder. *PeerJ.*, *6*, e5116. (2018). https://doi.org/10.7717/peerj.5116

Dallakyan, S., & Olson, A. J. (2015). Small-molecule library screening by docking with PyRx. In *Chemical biology* (pp. 243–250). Springer.

Darden, T., York, D., & Pedersen, L. (1993). Particle mesh Ewald: An N·log (N) method for Ewald sums in large systems. *The Journal of Chemical Physics*, *98*(12), 10089–10092. https://doi.org/10.1063/1.464397

Dash, R., Ali, M. C., Rana, M. L., Munni, Y. A., Barua, L., Jahan, I., Haque, M. F., Hannan, M. A., & Moon, I. S. (2020). Computational SNP analysis and molecular simulation revealed the most deleterious missense variants in the NBD1 domain of human ABCA1 transporter. *International Journal of Molecular Sciences*, *21*(20), 7606–7623. https://doi.org/10.3390/ijms21207606

Desai, M., & Chauhan, J. (2016). In silico analysis of nsSNPs in human methyl CpG binding protein 2. *Meta Gene*, *10*, 1–7. https://doi.org/10.1016/j.mgene.2016.09.004

Divanshu, G., Lekshmi, M., & Shanthi, V. (2014). In silico studies of deleterious non-synonymous single nucleotide polymorphisms (nsSNPs) of NRL gene. *Network Modeling Analysis in Health Informatics and Bioinformatics*, *3*(1), 1–7. https://doi.org/10.1007/s13721-014-0059-9

Drosten, C., Günther, S., Preiser, W., van der Werf, S., Brodt, H.-R., Becker, S., Rabenau, H., Panning, M., Kolesnikova, L., Fouchier, R. A. M., Berger, A., Burguière, A.-M., Cinatl, J., Eickmann, M., Escriou, N., Grywna, K., Kramme, S., Manuguerra, J.-C., Müller, S., … Doerr, H. W. (2003). Identification of a novel coronavirus in patients with severe acute respiratory syndrome. *The New England Journal of Medicine*, *348*(20), 1967–1976. https://doi.org/10.1056/NEJMoa030747

Ensembl.(2021). Ensembl. EMBL-EBI. http://uswest.ensembl.org/index.html

Ferrer-Costa, C., Gelpí, J. L., Zamakola, L., Parraga, I., De La Cruz, X., & Orozco, M. (2005). PMUT: A web-based tool for the annotation of pathological mutations on proteins. *Bioinformatics (Oxford, England)*, *21*(14), 3176–3178. https://doi.org/10.1093/bioinformatics/bti486

Frodsham, A. J., Zhang, L., Dumpis, U., Taib, N. A. M., Best, S., Durham, A., Hennig, B. J. W., Hellier, S., Knapp, S., Wright, M., Chiaramonte, M., Bell, J. I., Graves, M., Whittle, H. C., Thomas, H. C., Thursz, M. R., & Hill, A. V. S. (2006). Class II cytokine receptor gene cluster is a major locus for hepatitis B persistence. *Proceedings of the National Academy of Sciences of the United States of America*, *103*(24), 9148–9153. https://doi.org/10.1073/pnas.0602800103

Garrido-Martín, D., Borsari, B., Calvo, M., Reverter, F., & Guigó, R. (2021). Identification and analysis of splicing quantitative trait loci across multiple tissues in the human genome. *Nature Communications*, *12*(1),1-16. https://doi.org/10.1038/s41467-020-20578-2

Ghosh, R., Chakraborty, A., Biswas, A., & Chowdhuri, S. (2020a). Evaluation of green tea polyphenols as novel corona virus (SARS CoV-2) main protease (Mpro) inhibitors–an in silico docking and molecular dynamics simulation study. *Journal of Biomolecular Structure and Dynamics*, 1–13. https://doi.org/10.1080/07391102.2020.1779818

Ghosh, R., Chakraborty, A., Biswas, A., & Chowdhuri, S. (2020b). Identification of polyphenols from Broussonetia papyrifera as SARS CoV-2 main protease inhibitors using in silico docking and molecular dynamics simulation approaches. *Journal of Biomolecular Structure and Dynamics*, *0*(0), 1–14. https://doi.org/10.1080/07391102.2020.1802347

Hadjadj, J., Yatim, N., Barnabei, L., Corneau, A., Boussier, J., Smith, N., Péré, H., Charbit, B., Bondet, V., Chenevier-Gobeaux, C., Breillat, P., Carlier, N., Gauzit, R., Morbieu, C., Pène, F., Marin, N., Roche, N., Szwebel, T.-A., Merkling, S. H., … Terrier, B. (2020). Impaired type I interferon activity and inflammatory responses in severe COVID-19 patients. *Science (New York, N.Y.)*, *369*(6504), 718–724. https://doi.org/10.1126/science.abc6027

Hamosh, A., King, T. M., Rosenstein, B. J., Corey, M., Levison, H., Durie, P., Tsui, L.-C., McIntosh, I., Keston, M., & Brock, D. J. H. (1992). Cystic fibrosis patients bearing both the common missense mutation, Gly→ Asp at codon 551 and the ΔF508 mutation are clinically indistinguishable from ΔF508 homozygotes, except for decreased risk of meconium ileus. *American Journal of Human Genetics*, *51*(2), 245.

Havranek, B., & Islam, S. M. (2020). Prediction and evaluation of deleterious and disease causing non-synonymous SNPs (nsSNPs) in human NF2 gene responsible for neurofibromatosis type 2 (NF2). *Journal of Biomolecular Structure and Dynamics*, 1–12. https://doi.org/10.1080/07391102.2020.1805018

Hossain, M. S., Roy, A. S., & Islam, M. S. (2020). In silico analysis predicting effects of deleterious SNPs of human RASSF5 gene on its structure and functions. *Scientific Reports*, *10*(1), 1–14. https://doi.org/10.1038/s41598-020-71457-1

Hunter, S., Apweiler, R., Attwood, T. K., Bairoch, A., Bateman, A., Binns, D., Bork, P., Das, U., Daugherty, L., Duquenne, L., Finn, R. D., Gough, J., Haft, D., Hulo, N., Kahn, D., Kelly, E., Laugraud, A., Letunic, I., Lonsdale, D., … Yeats, C. (2009). InterPro: The integrative protein signature database. *Nucleic Acids Research*, *37*(Database), D211–215. https://doi.org/10.1093/nar/gkn785

Islam, M. J., Khan, A. M., Parves, M. R., Hossain, M. N., & Halim, M. A. (2019). Prediction of deleterious non-synonymous SNPs of human STK11 gene by combining algorithms, molecular docking, and molecular dynamics simulation. *Scientific Reports*, *9*(1), 1–16. https://doi.org/10.1038/s41598-019-52308-0

Islam, M. J., Parves, M. R., Mahmud, S., Tithi, F. A., & Reza, M. A. (2019). Assessment of structurally and functionally high-risk nsSNPs impacts on human bone morphogenetic protein receptor type IA (BMPR1A) by computational approach. *Computational Biology and Chemistry*, *80*, 31–45. https://doi.org/10.1016/j.compbiolchem.2019.03.004

Jennings, S. (2021). COVID-19 updates: US and global cases, deaths, and recoveries as of March 29, 2021. Patient Care. https://www.patientcareonline.com/view/covid-19-updates-us-and-global-cases-deaths-and-recoveries-as-of-march-29-2021

Krieger, E., Dunbrack, R. L., Hooft, R. W. W., & Krieger, B. (2012). Assignment of protonation states in proteins and ligands: Combining pK a prediction with hydrogen bonding network optimization. In *Computational Drug Discovery and Design* (pp. 405–421). Springer.

Krieger, E., Nielsen, J. E., Spronk, C. A. E. M., & Vriend, G. (2006). Fast empirical pKa prediction by Ewald summation. *Journal of Molecular Graphics & Modelling*, *25*(4), 481–486. https://doi.org/10.1016/j.jmgm.2006.02.009

Land, H., & Humble, M. S. (2018). YASARA: A tool to obtain structural guidance in biocatalytic investigations. In *Protein Engineering* (pp. 43–67). Springer.

Lee, J. S., & Shin, E.-C. (2020). The type I interferon response in COVID-19: Implications for treatment. *Nature Reviews. Immunology*, *20*(10), 585–586. https://doi.org/10.1038/s41577-020-00429-3

Lonsdale, J., Thomas, J., Salvatore, M., Phillips, R., Lo, E., Shad, S., Hasz, R., Walters, G., Garcia, F., Young, N., Foster, B., Moser, M., Karasik, E., Gillard, B., Ramsey, K., Sullivan, S., Bridge, J., Magazine, H., Syron, J., … Moore, H. F. (2013). The genotype-tissue expression (GTEx) project. *Nature Genetics*, *45*(6), 580–585. https://doi.org/10.1038/ng.2653

Lopez, A., Havranek, B., Papadantonakis, G. A., & Islam, S. M. (2021). In silico screening and molecular dynamics simulation of deleterious PAH mutations responsible for phenylketonuria genetic disorder. *Proteins: Structure, Function, and Bioinformatics*, *89*(6), 683–696. https://doi.org/10.1002/prot.26051

LoPresti, M., Beck, D. B., Duggal, P., Cummings, D. A. T., & Solomon, B. D. (2020). The role of host genetic factors in coronavirus susceptibility: review of animal and systematic review of human literature. *American Journal of Human Genetics*, *107*(3), 381–402. https://doi.org/10.1016/j.ajhg.2020.08.007

Marchler-Bauer, A., Derbyshire, M. K., Gonzales, N. R., Lu, S., Chitsaz, F., Geer, L. Y., Geer, R. C., He, J., Gwadz, M., Hurwitz, D. I., Lanczycki, C. J., Lu, F., Marchler, G. H., Song, J. S., Thanki, N., Wang, Z., Yamashita, R. A., Zhang, D., Zheng, C., & Bryant, S. H. (2015). CDD: NCBI's conserved domain database. *Nucleic Acids Research*, *43*(Database issue), D222–D226. https://doi.org/10.1093/nar/gku1221

Meyer, M. J., Lapcevic, R., Romero, A. E., Yoon, M., Das, J., Beltrán, J. F., Mort, M., Stenson, P. D., Cooper, D. N., Paccanaro, A., & Yu, H. (2016). mutation3D: Cancer gene prediction through atomic clustering of coding variants in the structural proteome. *Human Mutation*, *37*(5), 447–456. https://doi.org/10.1002/humu.22963

Mogil, L. S., Andaleon, A., Badalamenti, A., Dickinson, S. P., Guo, X., Rotter, J. I., Johnson, W. C., Im, H. K., Liu, Y., & Wheeler, H. E. (2018). Genetic architecture of gene expression traits across diverse populations. *PLoS Genetics*, *14*(8), e1007586. https://doi.org/10.1371/journal.pgen.1007586

Moszyńska, A., Gebert, M., Collawn, J. F., & Bartoszewski, R. (2017). SNPs in microRNA target sites and their potential role in human disease. *Open Biology*, *7*(4), 170019. https://doi.org/10.1098/rsob.170019

Nimir, M., Abdelrahim, M., Abdelrahim, M., Abdalla, M., Ahmed, W., Eldin, Abdullah, M., & Hamid, M. M. A. (2017). In silico analysis of single nucleotide polymorphisms (SNPs) in human FOXC2 gene. *F1000Research*, *6*(0), 243. https://doi.org/10.12688/f1000research.10937.1

Novick, D., Cohen, B., & Rubinstein, M. (1994). The human interferon alpha/beta receptor: characterization and molecular cloning. *Cell*, *77*(3), 391–400. https://doi.org/10.1016/0092-8674(94)90154-6

Oran, D. P., & Topol, E. J. (2020). Prevalence of asymptomatic SARS-CoV-2 infection : A narrative review. *Annals of Internal Medicine*, *173*(5), 362–367. https://doi.org/10.7326/m20-3012

Owji, H., Eslami, M., Nezafat, N., & Ghasemi, Y. (2020). In Silico Elucidation of Deleterious Non-synonymous SNPs in SHANK3, the Autism Spectrum Disorder Gene. *Journal of Molecular Neuroscience*, *70*(10), 1649–1667. https://doi.org/10.1007/s12031-020-01552-5

Pairo-Castineira, E., Clohisey, S., Klaric, L., Bretherick, A. D., Rawlik, K., Pasko, D., Walker, S., Parkinson, N., Fourman, M. H., Russell, C. D., Furniss, J., Richmond, A., Gountouna, E., Wrobel, N., Harrison, D., Wang, B., Wu, Y., Meynert, A., Griffiths, F., … Baillie, J. K., Gen-COVID Investigators. (2021). Genetic mechanisms of critical illness in Covid-19. *Nature*, *591*(7848), 92–98. https://doi.org/10.1038/s41586-020-03065-y

Pala, M., Zappala, Z., Marongiu, M., Li, X., Davis, J. R., Cusano, R., Crobu, F., Kukurba, K. R., Gloudemans, M. J., Reinier, F., Berutti, R., Piras, M. G., Mulas, A., Zoledziewska, M., Marongiu, M., Sorokin, E. P., Hess, G. T., Smith, K. S., Busonero, F., … Montgomery, S. B. (2017). Population- and individual-specific regulatory variation in Sardinia. *Nature Genetics*, *49*(5), 700–707. https://doi.org/10.1038/ng.3840

Pejaver, V., Urresti, J., Lugo-Martinez, J., Pagel, K. A., Lin, G. N., Nam, H. J., Mort, M., Cooper, D. N., Sebat, J., Iakoucheva, L. M., Mooney, S. D., & Radivojac, P. (2020). Inferring the molecular and phenotypic impact of amino acid variants with MutPred2. *Nature Communications*, *11*(1), 1–13. https://doi.org/10.1038/s41467-020-19669-x

Peleg, O., Choi, J.-M., & Shakhnovich, E. I. (2014). Evolution of specificity in protein-protein interactions. *Biophysical Journal*, *107*(7), 1686–1696. https://doi.org/10.1016/j.bpj.2014.08.004

Pettersen, E. F., Goddard, T. D., Huang, C. C., Couch, G. S., Greenblatt, D. M., Meng, E. C., & Ferrin, T. E. (2004). UCSF Chimera-a visualization system for exploratory research and analysis. *Journal of Computational Chemistry*, *25*(13), 1605–1612. https://doi.org/10.1002/jcc.20084

Purohit, R. (2014). Role of ELA region in auto-activation of mutant KIT receptor: A molecular dynamics simulation insight. *Journal of Biomolecular Structure & Dynamics*, *32*(7), 1033–1046. https://doi.org/10.1080/07391102.2013.803264

Ren, L.-L., Wang, Y.-M., Wu, Z.-Q., Xiang, Z.-C., Guo, L., Xu, T., Jiang, Y.-Z., Xiong, Y., Li, Y.-J., Li, X.-W., Li, H., Fan, G.-H., Gu, X.-Y., Xiao, Y., Gao, H., Xu, J.-Y., Yang, F., Wang, X.-M., Wu, C., … Wang, J.-W. (2020). Identification of a novel coronavirus causing severe pneumonia in

human: A descriptive study. *Chinese Medical Journal*, *133*(9), 1015–1024. https://doi.org/10.1097/CM9.0000000000000722

Rodriguez-Casado, A. (2012). In silico investigation of functional nsSNPs–an approach to rational drug design. *Research and Reports in Medicinal Chemistry*, *2*, 31–42. https://doi.org/10.2147/rrmc.s28211

Sadler, A. J., & Williams, B. R. G. (2008). Interferon-inducible antiviral effectors. *Nature Reviews. Immunology*, *8*(7), 559–568. https://doi.org/10.1038/nri2314

Sanner, M. F. (1999). Python: A programming language for software integration and development. *Journal of Molecular Graphics & Modelling*, *17*(1), 57–61.

Sen Gupta, P. S., Islam, R. N. U., Banerjee, S., Nayek, A., Rana, M. K., & Bandyopadhyay, A. K. (2020). Screening and molecular characterization of lethal mutations of human homogentisate 1, 2 dioxigenase. *Journal of Biomolecular Structure & Dynamics*, *39*(5), 1661–1671. https://doi.org/10.1080/07391102.2020.1736158

Sharma, J., Kumar Bhardwaj, V., Singh, R., Rajendran, V., Purohit, R., & Kumar, S. (2021). An in-silico evaluation of different bioactive molecules of tea for their inhibition potency against non structural protein-15 of SARS-CoV-2. *Food Chemistry*, *346*(January), 128933 https://doi.org/10.1016/j.foodchem.2020.128933

Sherry, S. T., Ward, M.-H., Kholodov, M., Baker, J., Phan, L., Smigielski, E. M., & Sirotkin, K. (2001). dbSNP: The NCBI database of genetic variation. *Nucleic Acids Res*, *29*(1), 308–311. https://doi.org/10.1093/nar/29.1.308

Sim, N.-L., Kumar, P., Hu, J., Henikoff, S., Schneider, G., & Ng, P. C. (2012). SIFT web server: Predicting effects of amino acid substitutions on proteins. *Nucleic Acids Research*, *40*(Web Server issue), W452–W457. https://doi.org/10.1093/nar/gks539

Trott, O., & Olson, A. J. (2010). AutoDock Vina: Improving the speed and accuracy of docking with a new scoring function, efficient optimization, and multithreading. *Journal of Computational Chemistry*, *31*(2), 455–461. https://doi.org/10.1002/jcc.21334

UniProt. (2021). UniProtKB - P48551 (INAR2_HUMAN). UniProt. https://www.uniprot.org/uniprot/P48551

van der Made, C. I., Simons, A., Schuurs-Hoeijmakers, J., van den Heuvel, G., Mantere, T., Kersten, S., van Deuren, R. C., Steehouwer, M., van Reijmersdal, S. V., Jaeger, M., Hofste, T., Astuti, G., Corominas Galbany, J., van der Schoot, V., van der Hoeven, H., Hagmolen Of ten Have, W., Klijn, E., van den Meer, C., Fiddelaers, J., … Hoischen, A. (2020). Presence of genetic variants among young men with severe COVID-19. *Jama - Jama*, *324*(7), 663–673. https://doi.org/10.1001/jama.2020.13719

Venselaar, H., Te Beek, T. A., Kuipers, R. K., Hekkelman, M. L., & Vriend, G. (2010). Protein structure analysis of mutations causing inheritable diseases. An e-Science approach with life scientist friendly interfaces. *BMC Bioinformatics*, *11*(1), 548. https://doi.org/10.1186/1471-2105-11-548

Wang, Q., He, J., Wu, D., Wang, J., Yan, J., & Li, H. (2015). Interaction of α-cyperone with human serum albumin: Determination of the binding site by using Discovery Studio and via spectroscopic methods. *Journal of Luminescence*, *164*, 81–85. https://doi.org/10.1016/j.jlumin.2015.03.025

Westra, H. J., & Franke, L. (2014). From genome to function by studying eQTLs. *Biochimica et Biophysica Acta*, *1842*(10), 1896–1902. https://doi.org/10.1016/j.bbadis.2014.04.024

WHO. (2020a). *Naming the coronavirus disease (COVID-19) and the virus that causes it*.

WHO. (2020b). *World Health Organization coronavirus disease (COVID-19) dashboard*.

Xu, Y., Wang, H., Nussinov, R., & Ma, B. (2013). Protein charge and mass contribute to the spatio-temporal dynamics of protein–protein interactions in a minimal proteome. *PROTEOMICS*, *13*(8), 1339–1351. https://doi.org/10.1002/pmic.201100540

Zhang, Q., Bastard, P., Liu, Z., Le Pen, J., Moncada-Velez, M., Chen, J., Ogishi, M., Sabli, I. K. D., Hodeib, S., Korol, C., Rosain, J., Bilguvar, K., Ye, J., Bolze, A., Bigio, B., Yang, R., Arias, A. A., Zhou, Q., Zhang, Y., … Casanova, J.-L, COVID-STORM Clinicians† (2020). Inborn errors of type I IFN immunity in patients with life-threatening COVID-19. *Science*, *370*(6515), eabd4570. https://doi.org/10.1126/science.abd4570

Zhang, M., Huang, C., Wang, Z., Lv, H., & Li, X. (2020). In silico analysis of non-synonymous single nucleotide polymorphisms (nsSNPs) in the human GJA3 gene associated with congenital cataract. *BMC Molecular and Cell Biology*, *21*(1), 12–13. https://doi.org/10.1186/s12860-020-00252-7

Zhu, N., Zhang, D., Wang, W., Li, X., Yang, B., Song, J., Zhao, X., Huang, B., Shi, W., Lu, R., Niu, P., Zhan, F., Ma, X., Wang, D., Xu, W., Wu, G., Gao, G. F., & Tan, W, China Novel Coronavirus Investigating and Research Team. (2020). A novel Coronavirus from patients with pneumonia in China, 2019. *The New England Journal of Medicine*, *382*(8), 727–733. https://doi.org/10.1056/NEJMoa2001017

Zou, J., Castro, R., & Tafalla, C. (2016). Antiviral immunity: Origin and evolution in vertebrates. In *The Evolution of the Immune System: Conservation and Diversification* (pp. 173–204). https://doi.org/10.1016/B978-0-12-801975-7.00007-4